



*Supplement of*

## **Variable organic matter stoichiometry enhances the biological drawdown of CO<sub>2</sub> in the northwest European shelf seas**

Kubilay Timur Demir et al.

*Correspondence to:* Kubilay Timur Demir (kubilay.demir@hereon.de)

The copyright of individual parts of the supplement might differ from the article licence.

## S1 Supplementary Figures and Tables

### S1.1 Supplementary Figures

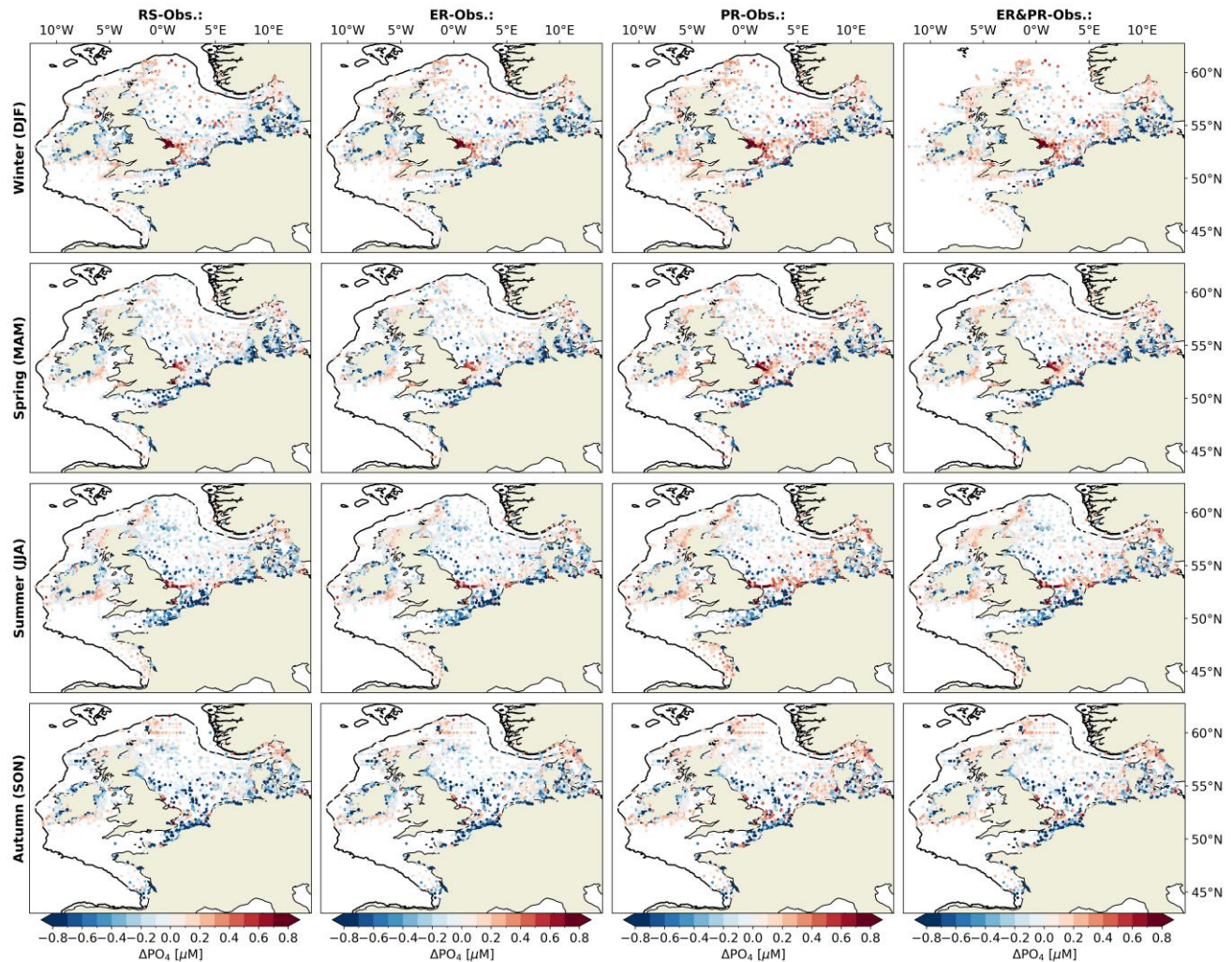


**Figure S1:** Differences between simulated and observed seasonal phosphate ( $\text{PO}_4$ ) concentrations over 2000–2010. The total of 161,152 data points from the International Council for the Exploration of the Sea (ICES) are compared to respective model output, co-located by a horizontal and vertical nearest neighbor search, for all four configurations: Redfield Stoichiometry (RS), Extracellular Release (ER), Preferential Remineralization (PR), and the combined configuration (ER&PR). The data includes both bottle and pump data from the ocean hydrochemistry data collection.

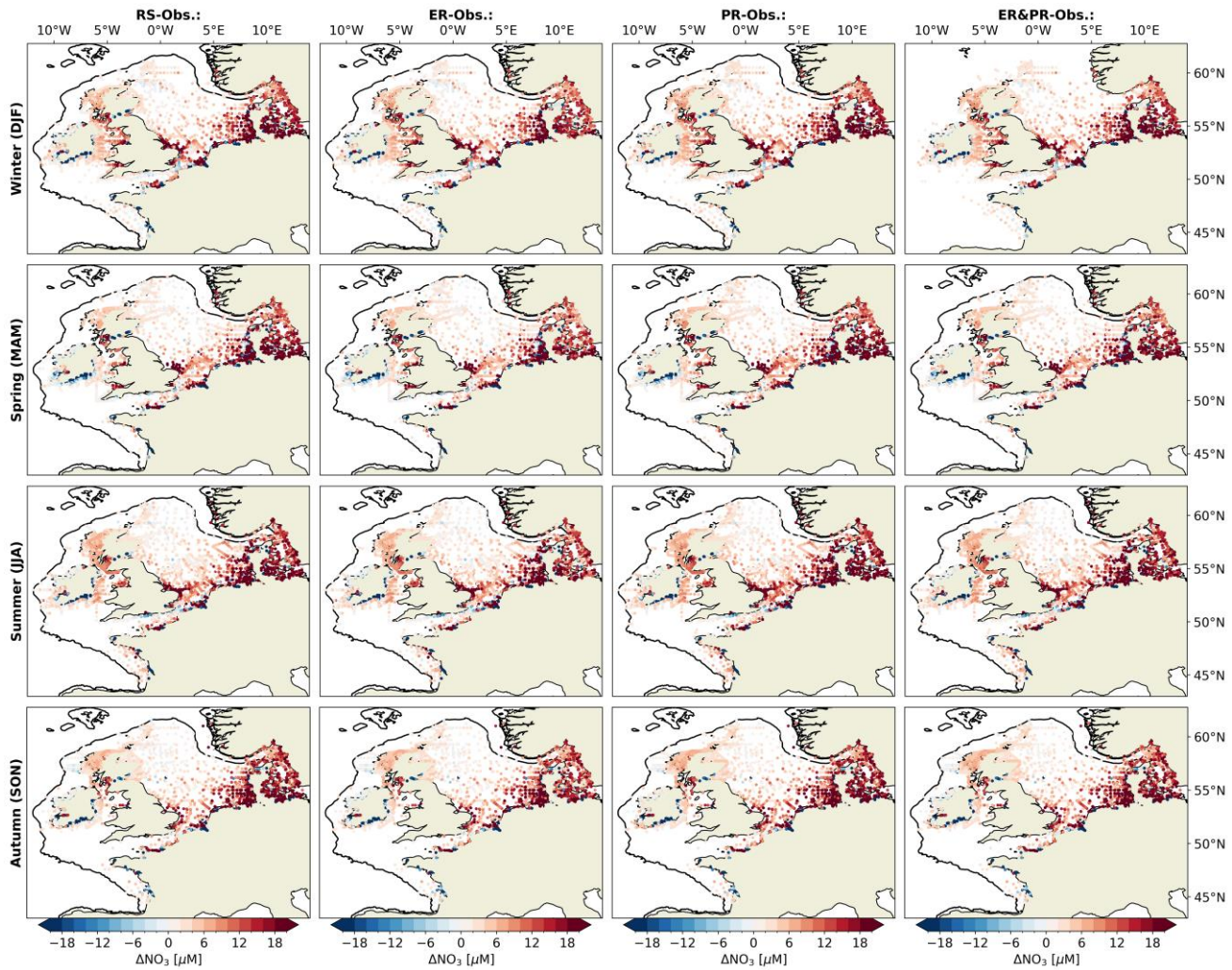


**Figure S2:** Differences between simulated and observed seasonal nitrate ( $\text{NO}_3$ ) concentrations over 2000–2010. The total of 135,469 data points from the International Council for the Exploration of the Sea (ICES) are compared to respective model output, co-located by a horizontal and vertical nearest neighbor search, for all four configurations: Redfield Stoichiometry (RS), Extracellular Release (ER), Preferential Remineralization (PR), and the combined configuration (ER&PR). The data includes both bottle and pump data from the ocean hydrochemistry data collection.

### RS-Obs.:

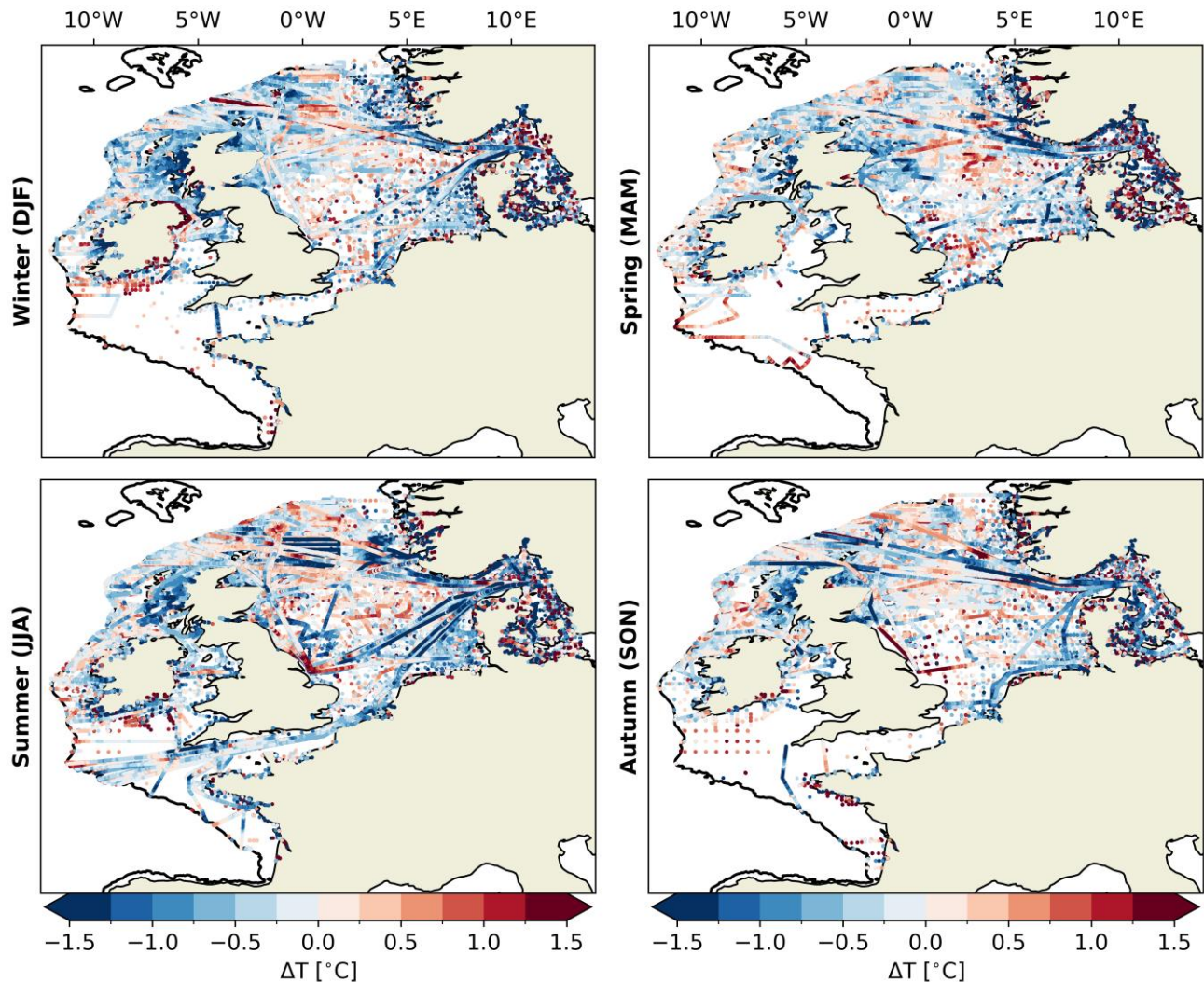


**Figure S3:** Differences between simulated and observed seasonal in situ temperature (T) over 2000–2010. The total of 2,153,726 data points from the International Council for the Exploration of the Sea (ICES) are compared to respective model output, co-located by a horizontal and vertical nearest neighbor search for the Redfield Stoichiometry (RS) configuration. As the physical simulation is consistent between all four simulations, it is not shown for each of the configurations. The data includes the surface, bottle, and pump data from the ocean hydrochemistry data collection.

### RS-Obs.:

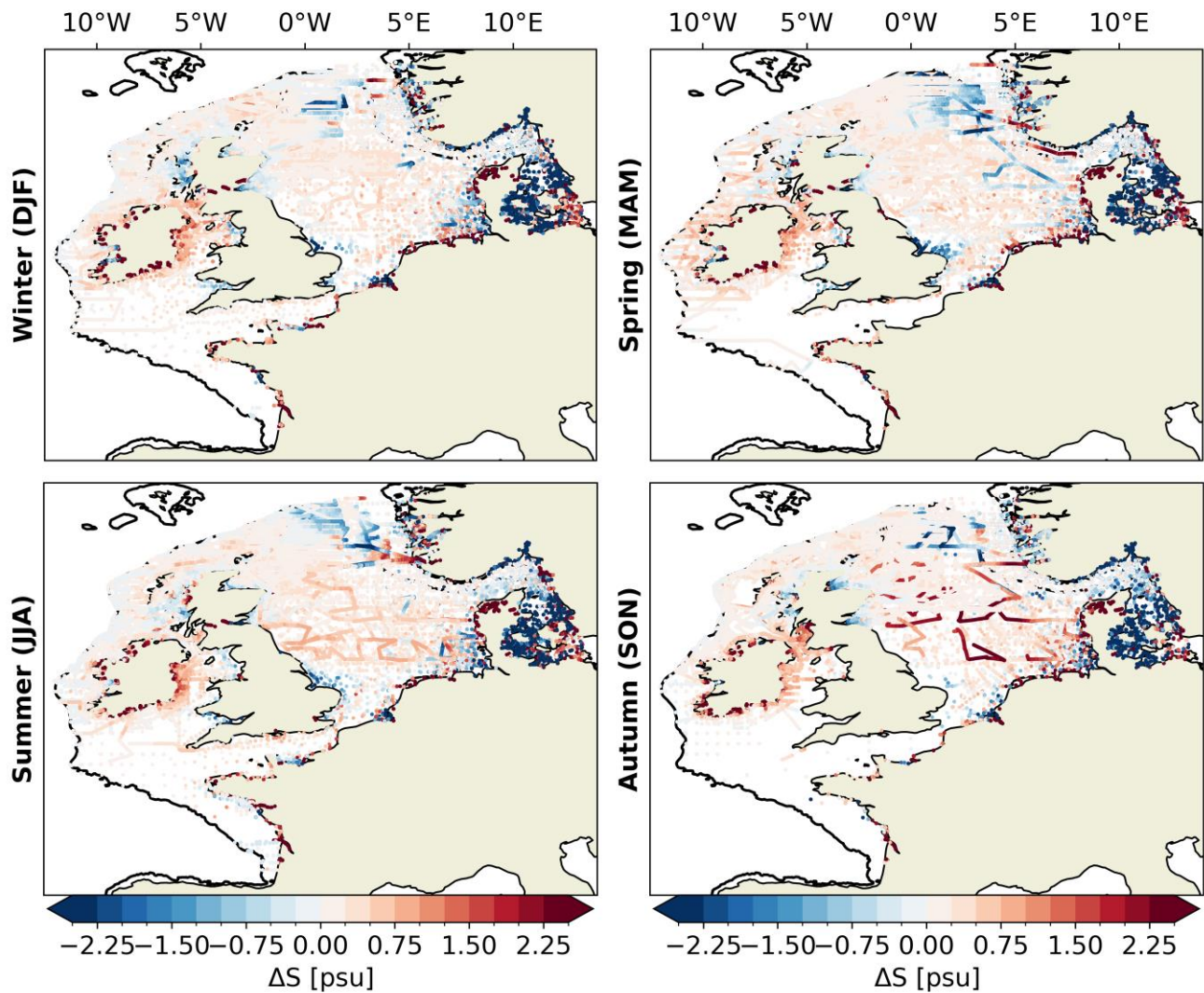


**Figure S4:** Differences between simulated and observed seasonal salinity ( $S$ ) over 2000–2010. The total of 1,913,297 data points from the International Council for the Exploration of the Sea (ICES) are compared to respective model output, co-located by a horizontal and vertical nearest neighbor search for the Redfield Stoichiometry (RS) configuration. As the physical simulation is consistent between all four simulations, it is not shown for each of the configurations. The data includes the bottle and pump data from the ocean hydrochemistry data collection.

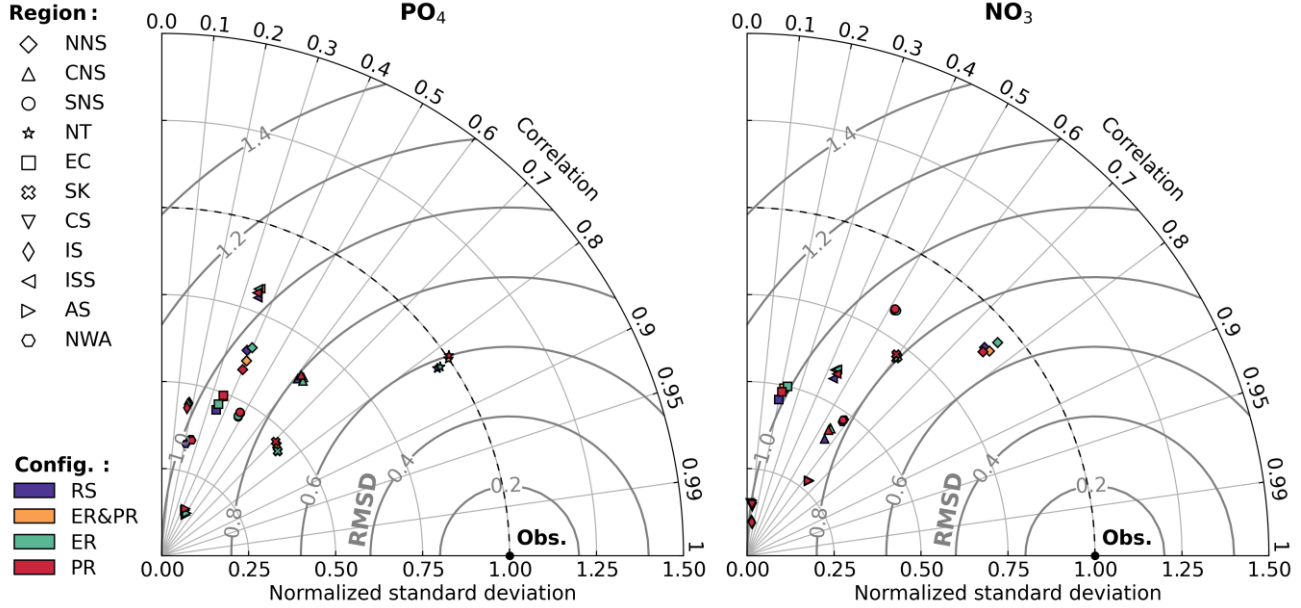


**Figure S5:** Taylor diagrams for phosphate ( $\text{PO}_4$ ) and nitrate ( $\text{NO}_3$ ), both limiting nutrients for primary production, showing correlation, root mean squared difference (RMSD), and normalized standard deviation of the model output with respect to observations. For each of the variables, the respective observations from Figures S1 and S2 are combined for all seasons and compared to the co-located model output using a horizontal and vertical nearest neighbor search. The model performance is differentiated by configuration, as indicated by color, and subregion, as indicated by shape.

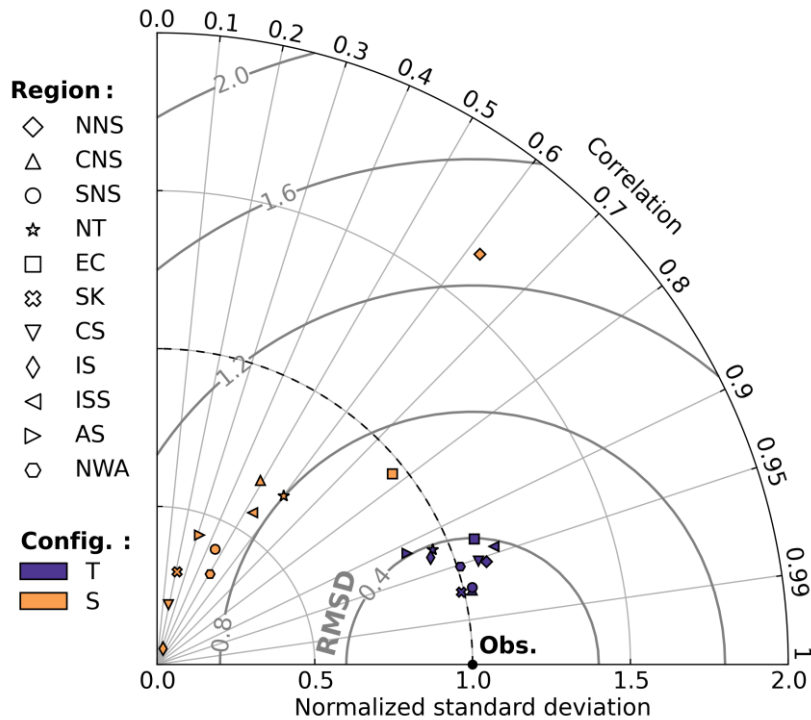


**Figure S6:** Taylor diagrams for the physical variables in situ temperature (T) and salinity (S), showing correlation, root mean squared difference (RMSD), and normalized standard deviation of the model output with respect to observations. For each of the variables, the respective observations from Figures S3 and S4 are combined for all seasons and compared to the co-located model output. As all four physical model configurations are consistent, we here only show the results for the Redfield Stoichiometry (RS) configuration.

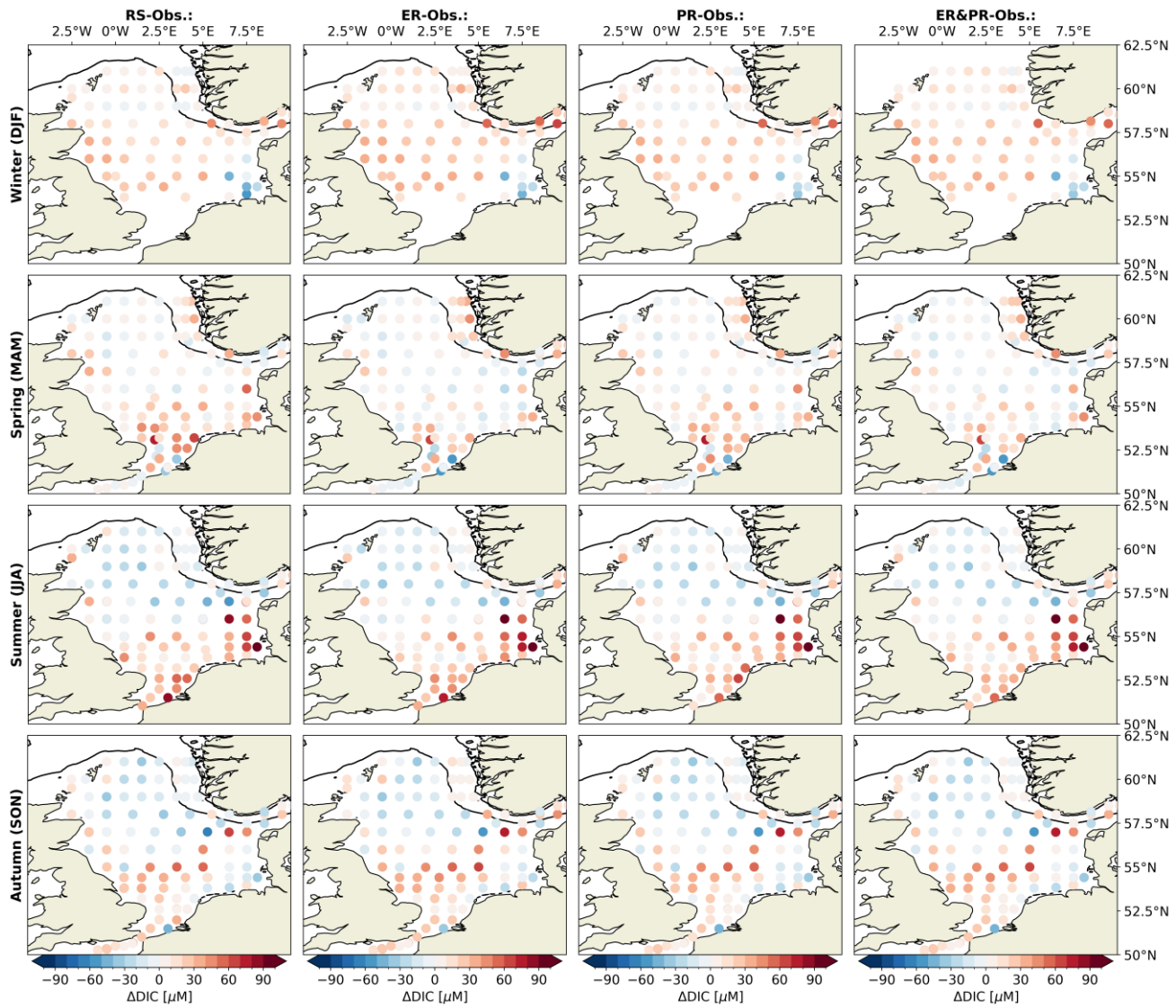


**Figure S7:** Differences between simulated and observed seasonal dissolved inorganic carbon (DIC) concentrations over 2000–2010. The total of 5,685 data points from the Global Ocean Data Analysis Project (GLODAP) are compared to respective model output, co-located by a horizontal and vertical nearest neighbor search, for all four configurations: Redfield Stoichiometry (RS), Extracellular Release (ER), Preferential Remineralization (PR), and the combined configuration (ER&PR).

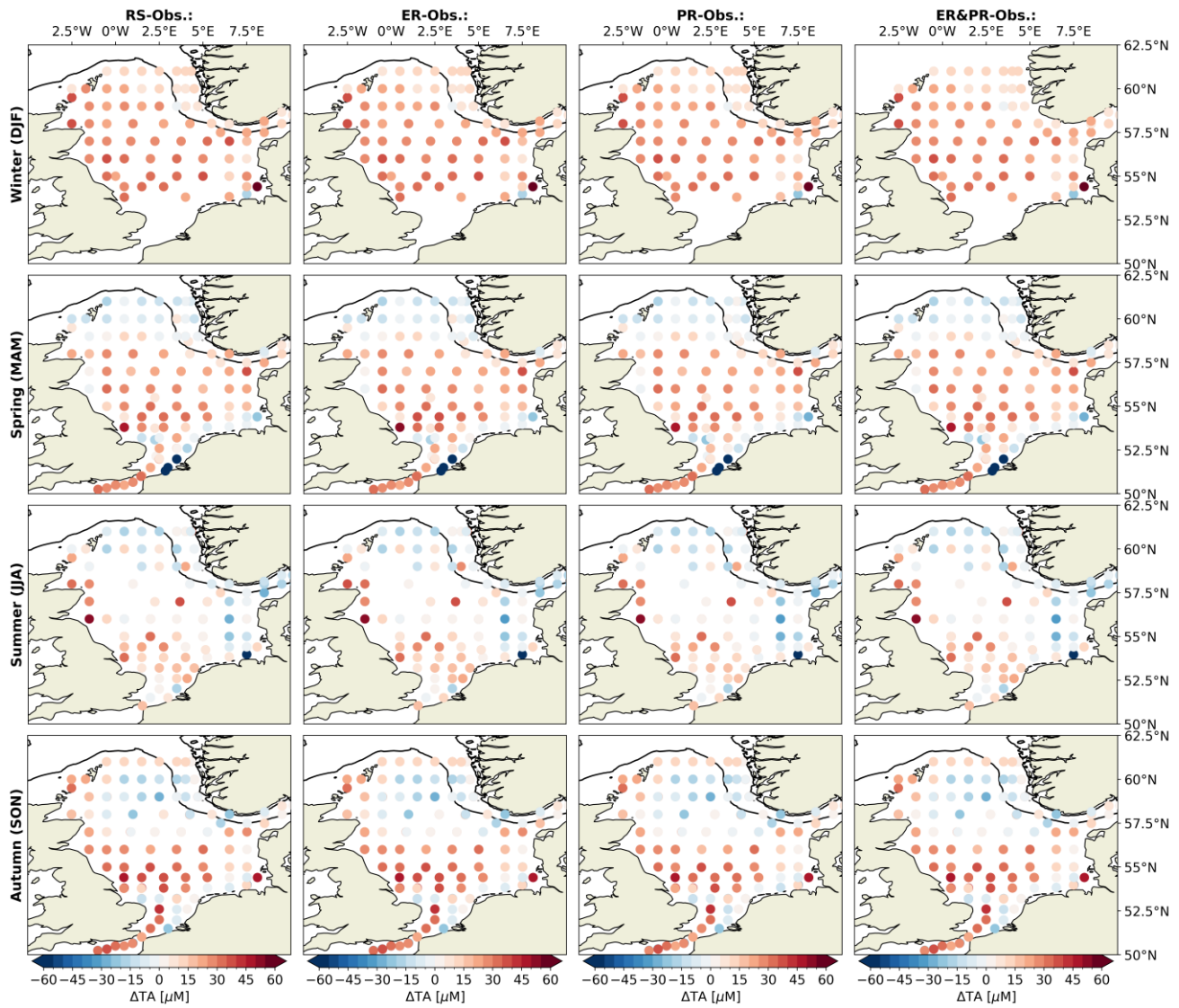


**Figure S8:** Differences between simulated and observed seasonal total alkalinity (TA) over 2000–2010. The total of 5,110 data points from the Global Ocean Data Analysis Project (GLODAP) are compared to respective model output, co-located by a horizontal and vertical nearest neighbor search, for all four configurations: Redfield Stoichiometry (RS), Extracellular Release (ER), Preferential Remineralization (PR), and the combined configuration (ER&PR).

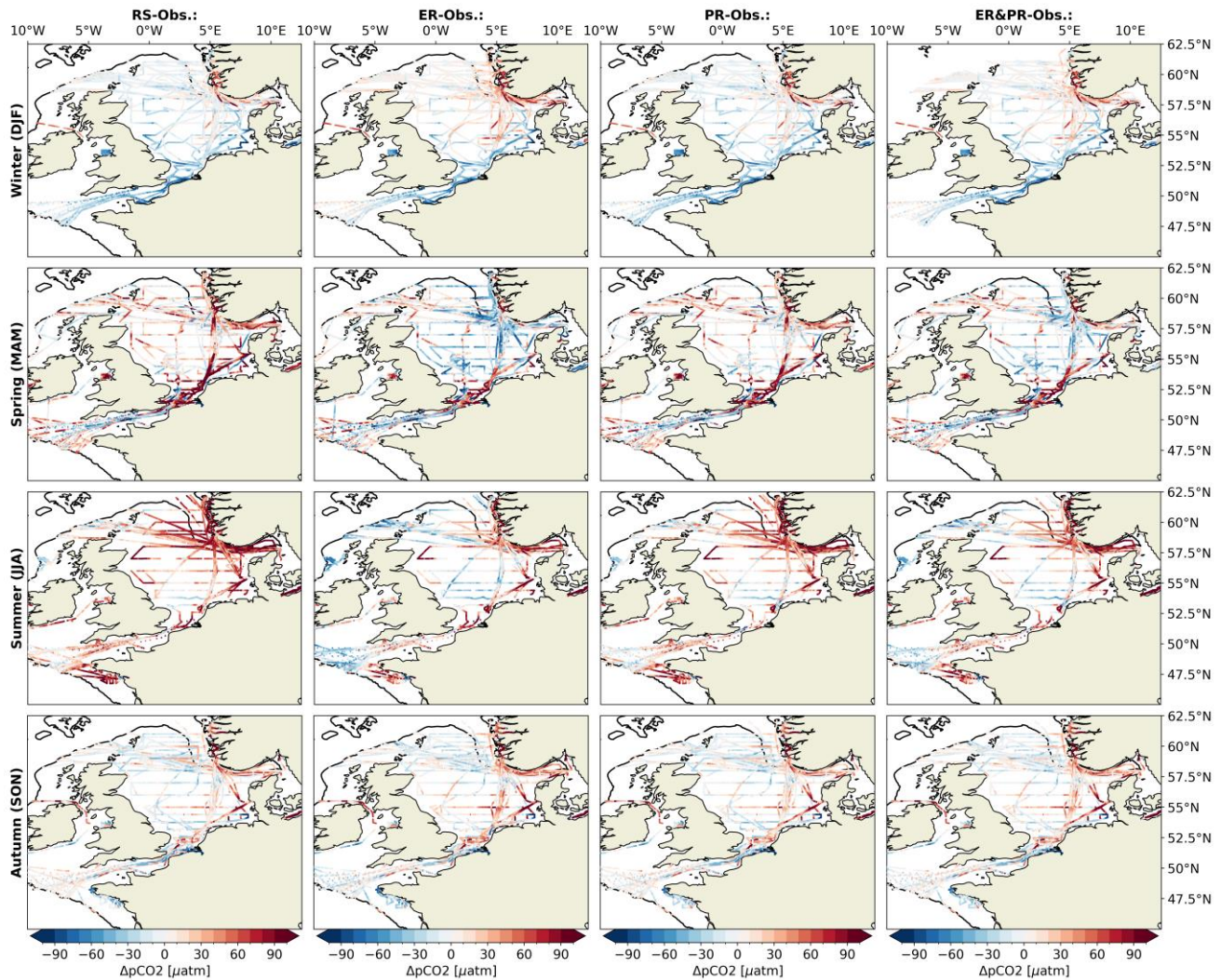


**Figure S9:** Differences between simulated and observed seasonal surface partial pressure of  $\text{CO}_2$  ( $\text{pCO}_2$ ) over 2000–2010. The total of 772,202 data points in the northwest European shelf seas from the Surface Ocean  $\text{CO}_2$  Atlas (SOCAT) are compared to respective model output, co-located by a horizontal nearest neighbor search, for all four configurations: Redfield Stoichiometry (RS), Extracellular Release (ER), Preferential Remineralization (PR), and the combined configuration (ER&PR). Observations were converted from  $\text{fCO}_2$  to  $\text{pCO}_2$  using PyCO2SYS (Humphreys et al., 2022, 2024). Model  $\text{CO}_2$  concentrations in parts per million were converted to  $\text{pCO}_2$  using Eq. 15–16, based on the conversion suggested by PyCO2SYS (Humphreys et al., 2022, 2024) and an improved temperature-dependent saturation vapor pressure equation (Huang, 2018).

### Annual Vertically-Integrated Subarea Carbon Fixation

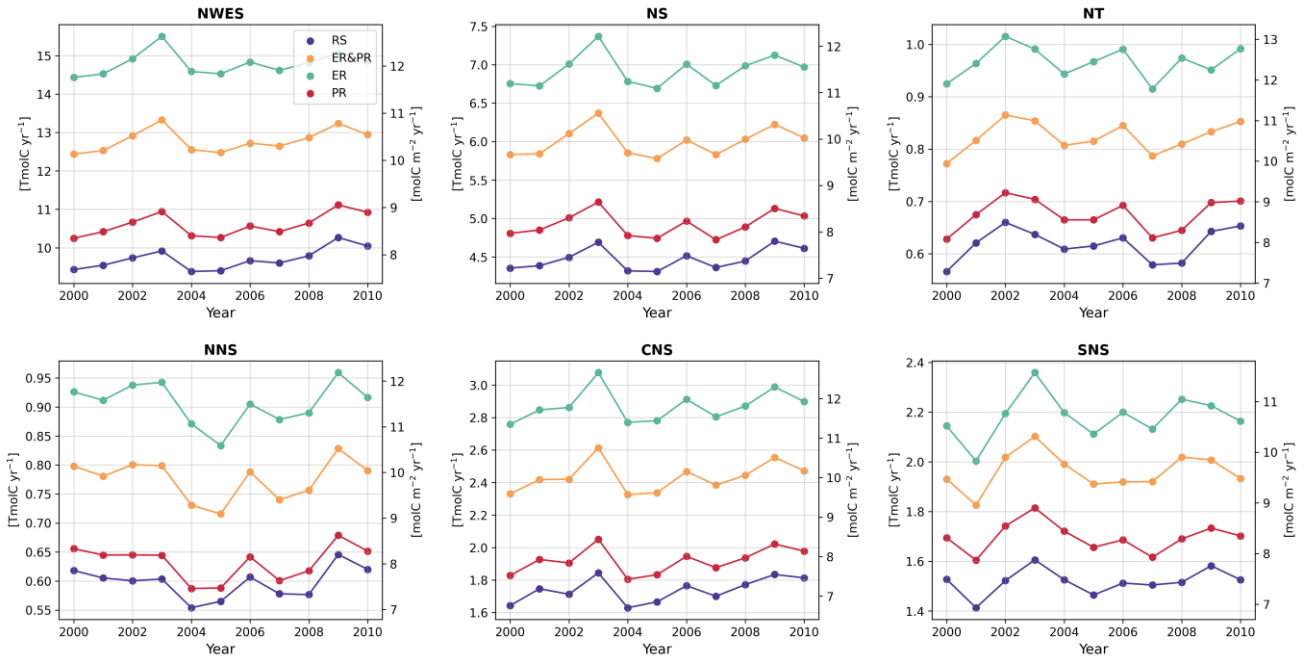


**Figure S10:** Time Series of annual vertically-integrated carbon fixation for the entire northwest European shelf seas (NWES), the North Sea (NS), the Norwegian Trench (NT), and the northern, central and southern North Sea (NNS, CNS, SNS). These include all four configurations: Redfield Stoichiometry (RS), Extracellular Release (ER), Preferential Remineralization (PR), and the combined configuration (ER&PR).

### Annual Vertically-Integrated Subarea Pelagic Carbon Remineralization

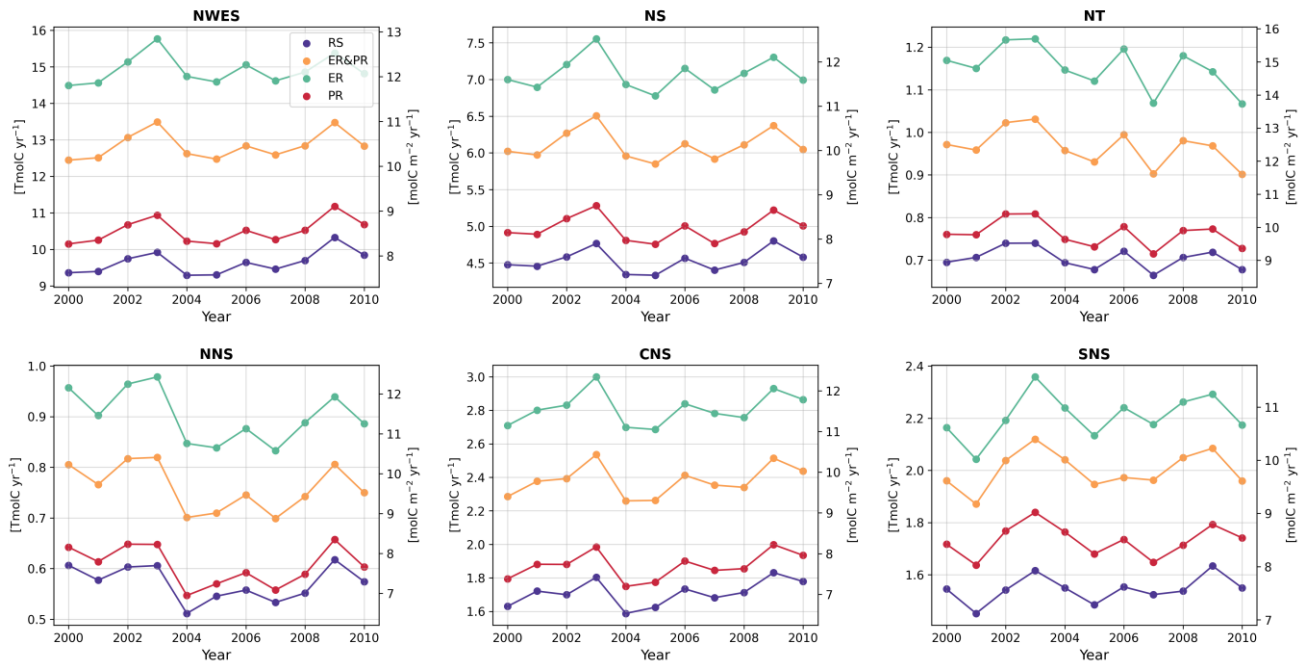


**Figure S11:** Time Series of annual vertically-integrated pelagic carbon remineralization for the entire northwest European shelf seas (NWES), the North Sea (NS), the Norwegian Trench (NT), and the northern, central and southern North Sea (NNS, CNS, SNS). These include all four configurations: Redfield Stoichiometry (RS), Extracellular Release (ER), Preferential Remineralization (PR), and the combined configuration (ER&PR).

### Annual Subarea-Integrated Benthic Carbon Remineralization

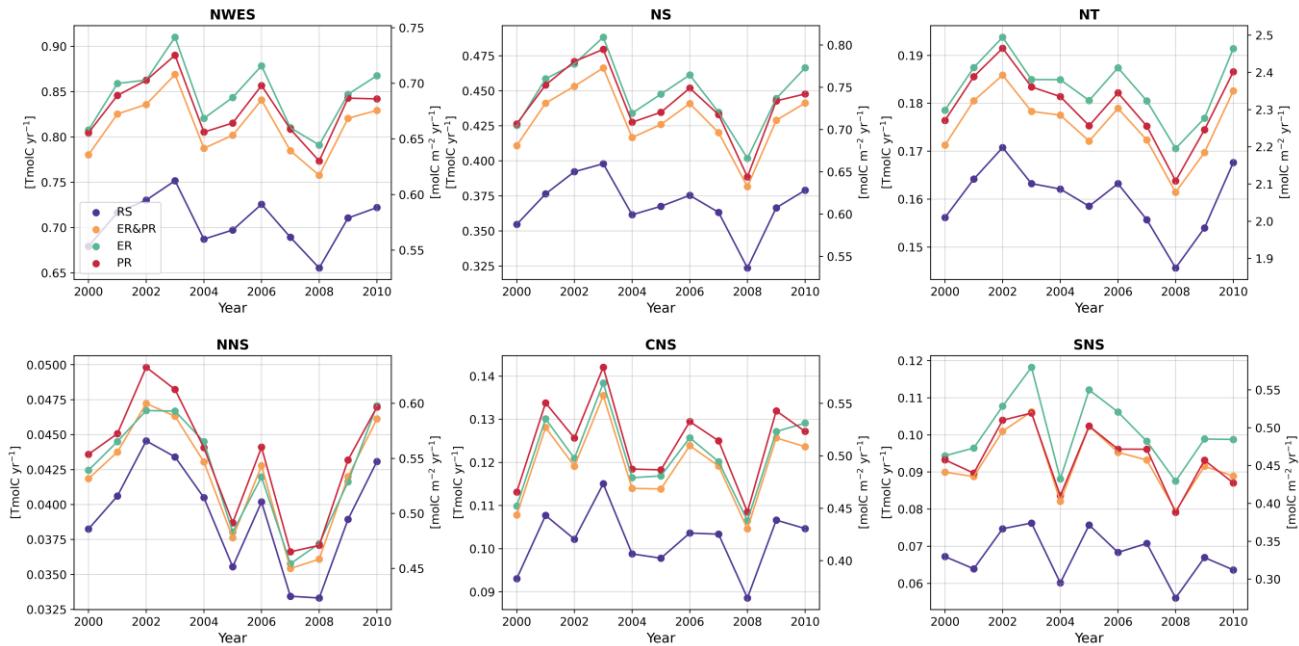


**Figure S12:** Time Series of annual subarea-integrated benthic carbon remineralization for the entire northwest European shelf seas (NWES), the North Sea (NS), the Norwegian Trench (NT), and the northern, central and southern North Sea (NNS, CNS, SNS). These include all four configurations: Redfield Stoichiometry (RS), Extracellular Release (ER), Preferential Remineralization (PR), and the combined configuration (ER&PR).

### Annual Vertically-Integrated Subarea Net Community Production

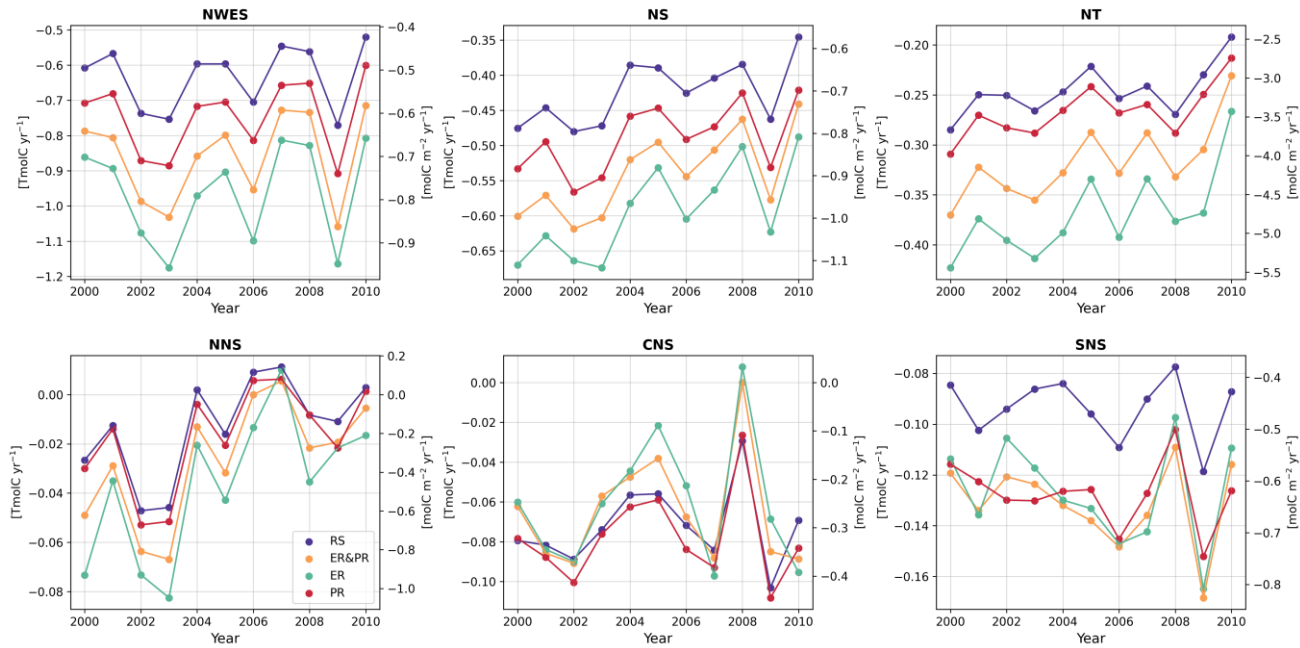


**Figure S13:** Time Series of annual vertically-integrated net community production for the entire northwest European shelf seas (NWES), the North Sea (NS), the Norwegian Trench (NT), and the northern, central and southern North Sea (NNS, CNS, SNS). These include all four configurations: Redfield Stoichiometry (RS), Extracellular Release (ER), Preferential Remineralization (PR), and the combined configuration (ER&PR).

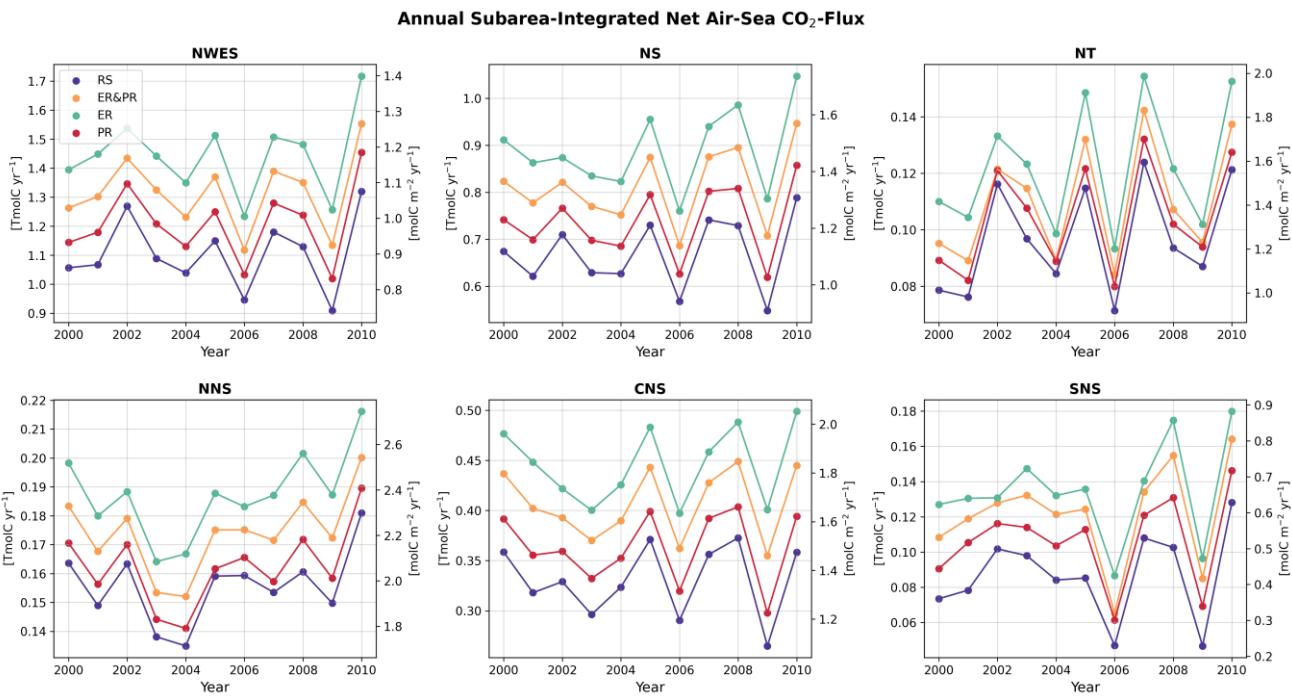


**Figure S14:** Time Series of subarea-integrated annual net air-sea CO<sub>2</sub> flux for the entire northwest European shelf seas (NWES), the North Sea (NS), the Norwegian Trench (NT), and the northern, central and southern North Sea (NNS, CNS, SNS). These include all four configurations: Redfield Stoichiometry (RS), Extracellular Release (ER), Preferential Remineralization (PR), and the combined configuration (ER&PR).

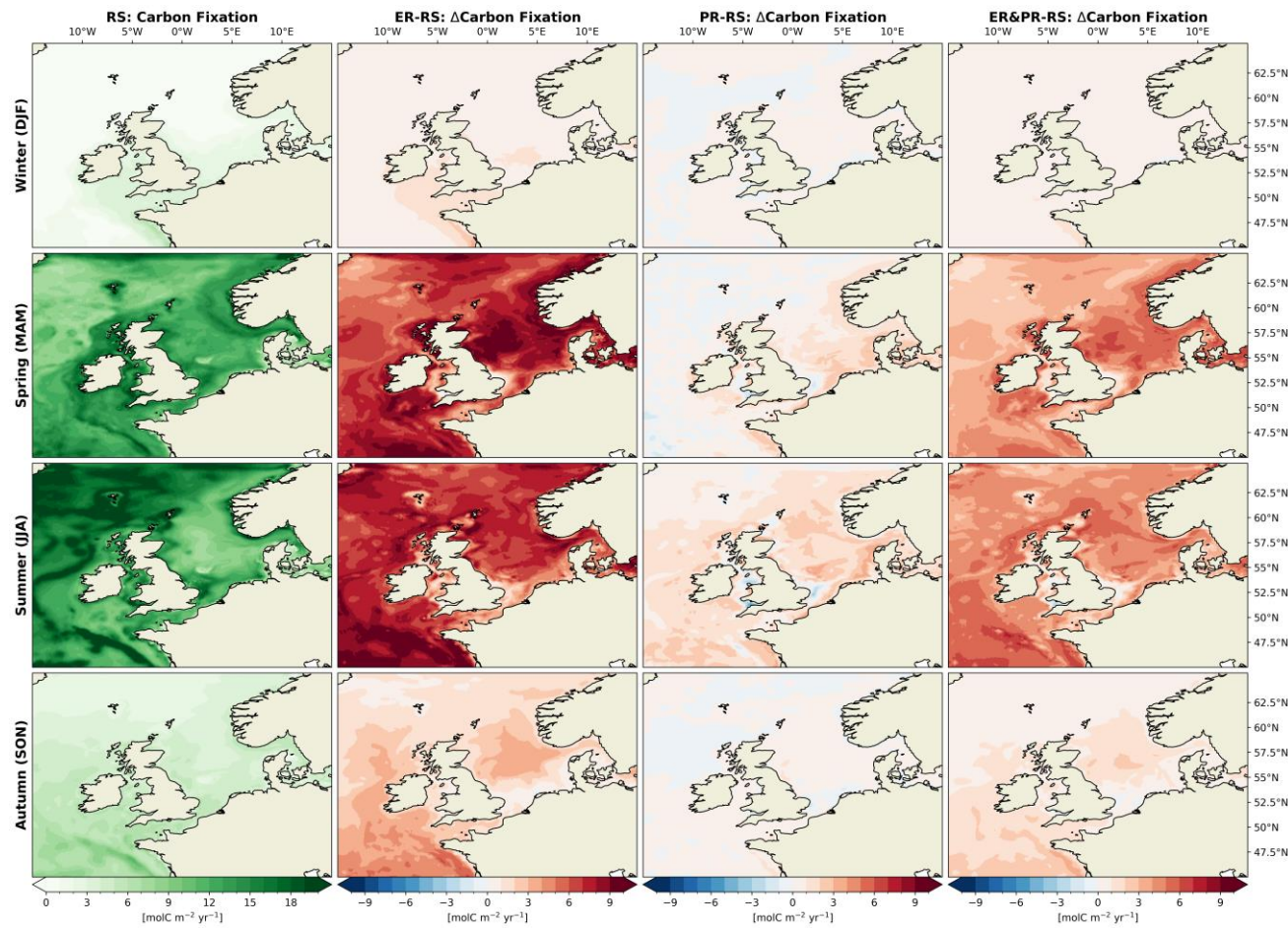


**Figure S15:** Simulated spatial distribution of seasonal means of vertically-integrated carbon fixation for the Redfield Stoichiometry (RS) configuration and differences for the Extracellular Release (ER), Preferential Remineralization (PR), and the combined (ER&PR) configurations. In the ER and ER&PR configurations, the carbon fixation includes the extracellular release of DOC.

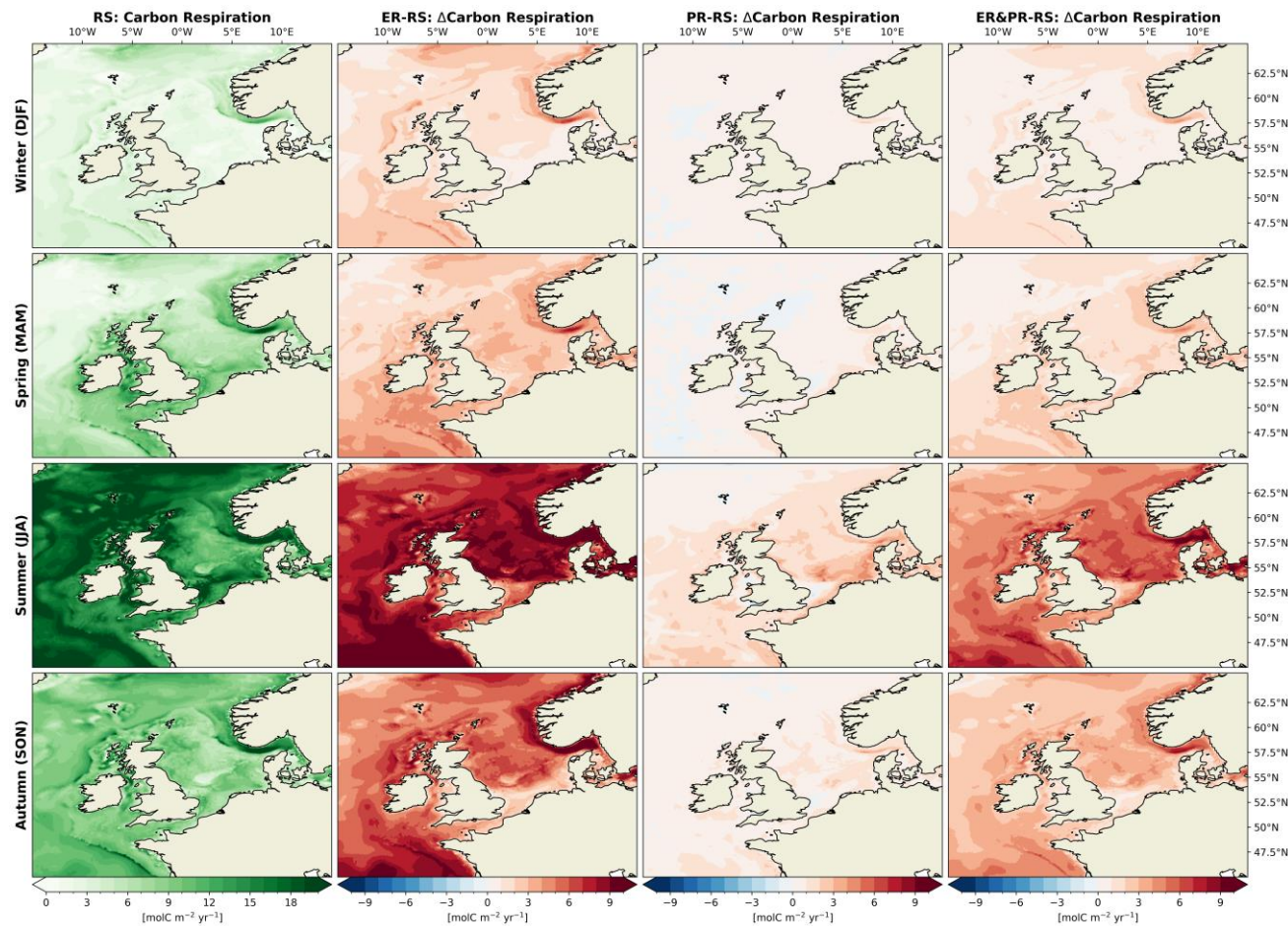


**Figure S16:** Simulated spatial distribution of seasonal means of vertically-integrated carbon respiration for the Redfield Stoichiometry (RS) configuration and differences for the Extracellular Release (ER), Preferential Remineralization (PR), and the combined (ER&PR) configurations. Carbon respiration here includes both pelagic and benthic heterotrophic remineralization.

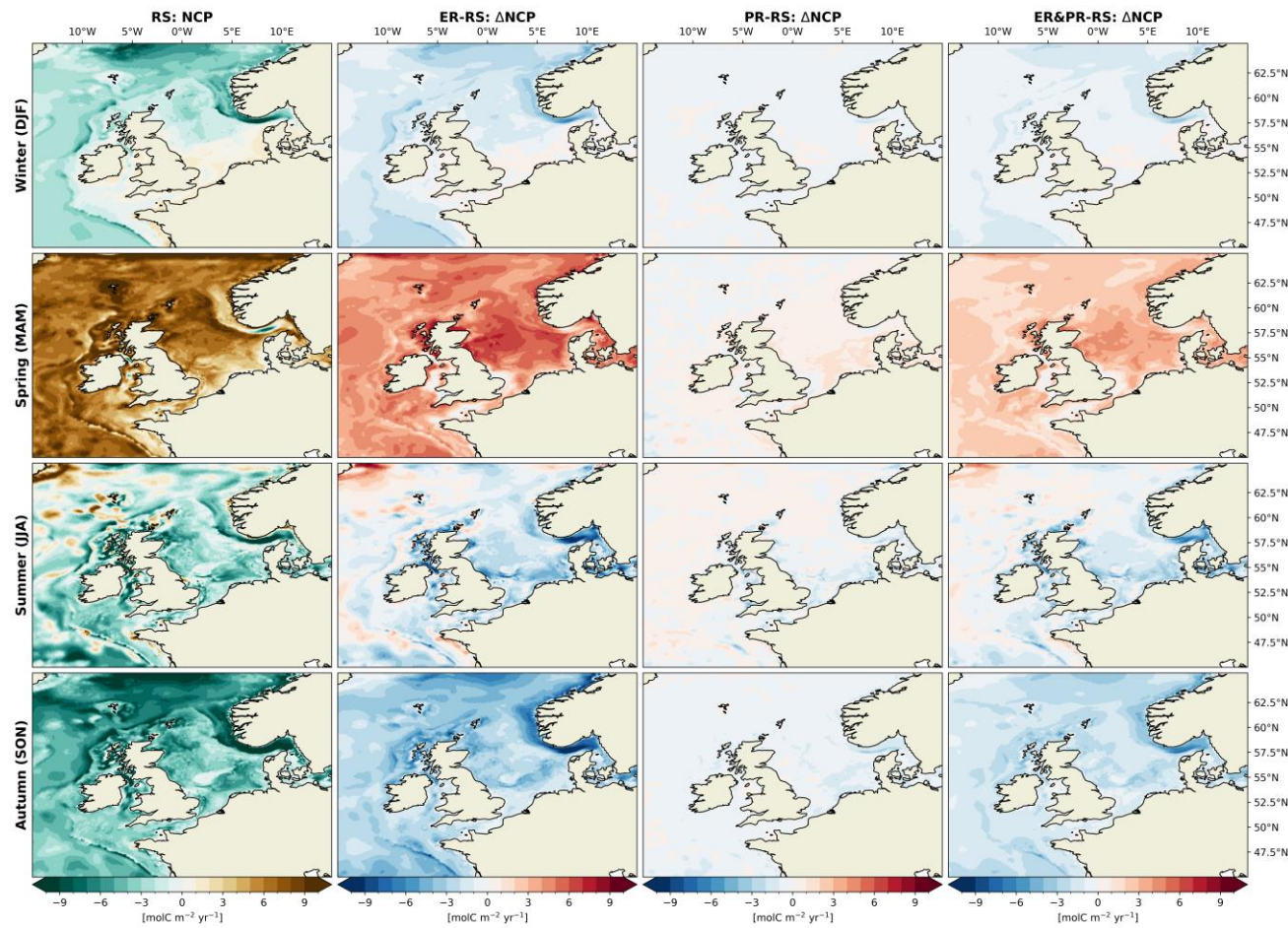


**Figure S17:** Simulated spatial distribution of seasonal means of vertically-integrated net community production (NCP) for the Redfield Stoichiometry (RS) configuration and differences for the Extracellular Release (ER), Preferential Remineralization (PR), and the combined (ER&PR) configurations. Net community production is here defined as carbon fixation minus respiration, where carbon respiration includes both pelagic and benthic heterotrophic remineralization.

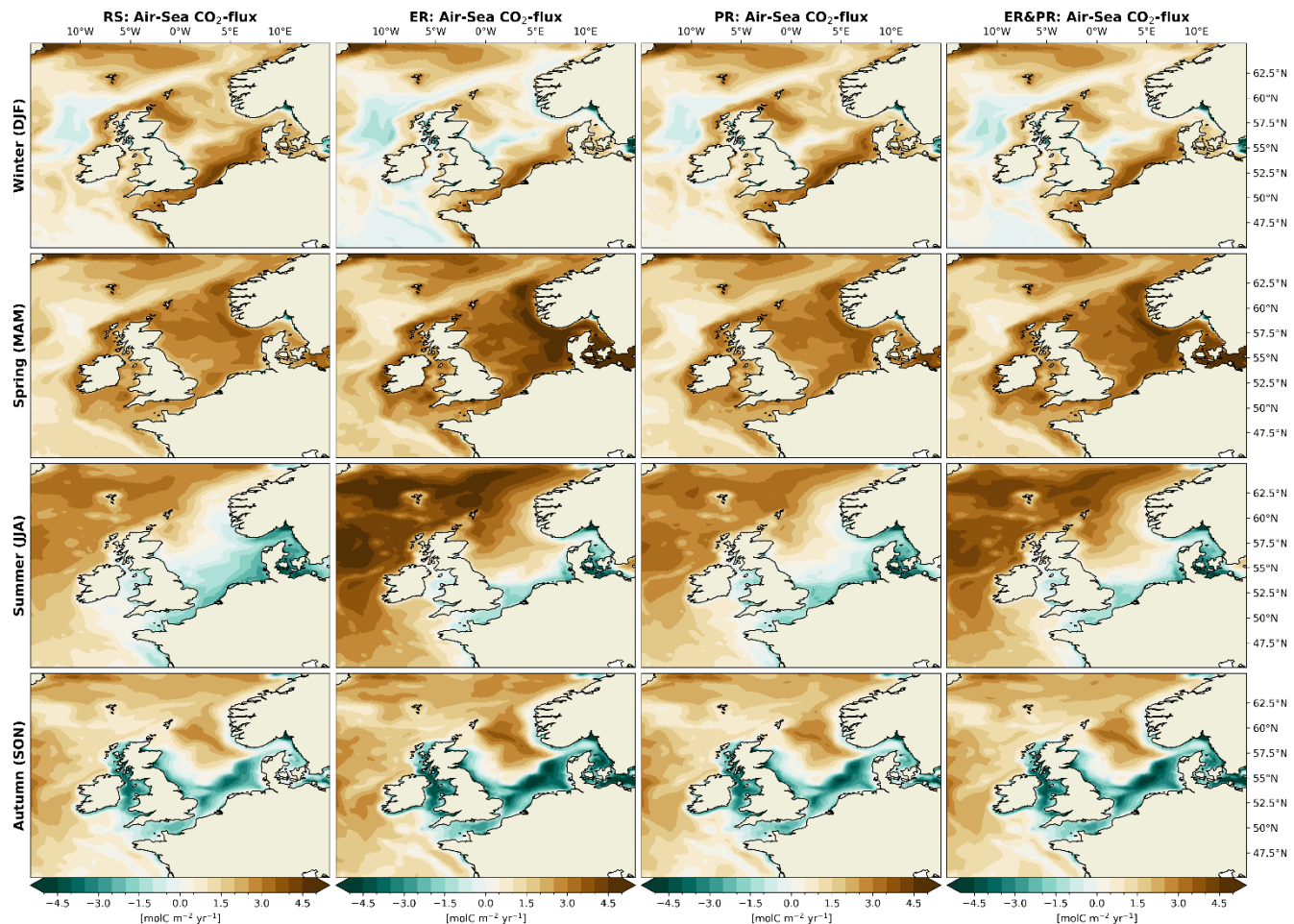


**Figure S18:** Simulated spatial distribution of the respective seasonal means of the air-sea  $\text{CO}_2$  exchange for all four configurations: the Redfield Stoichiometry (RS), Extracellular Release (ER), Preferential Remineralization (PR), and the combined (ER&PR) configuration.

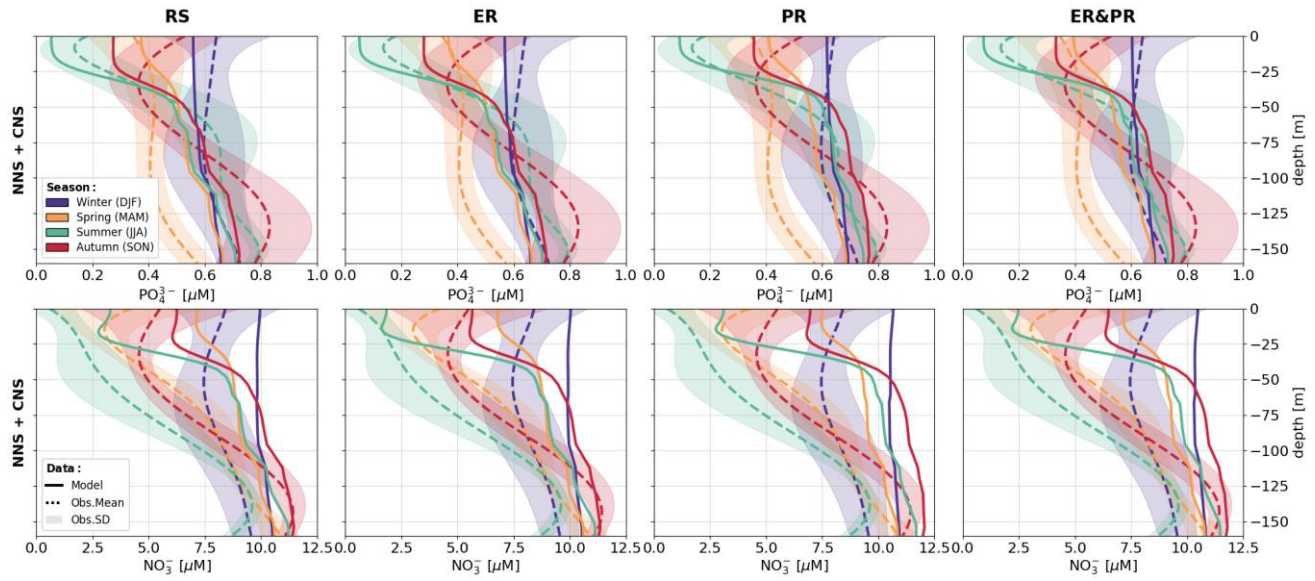


**Figure S19:** Vertical distribution of observed and simulated, seasonally and subarea-averaged  $\text{NO}_3^-$  and  $\text{PO}_4^{3-}$  concentrations for all four model configurations: Redfield Stoichiometry (RS), Extracellular Release (ER), Preferential Remineralization (PR), and the combined configuration (ER&PR). Both model output and observational data are averages over the simulated period 2000–2010 for the respective season. For the combined Northern (NNS) and central North Sea (CNS) sub-regions 11,636 and 11,065 data points were selected for  $\text{PO}_4^{3-}$  and  $\text{NO}_3^-$  respectively from the bottle and pump data in the ocean hydrochemistry data collection of the International Council for the Exploration of the Sea (ICES). The vertical profiles were generated by firstly calculating the mean concentrations and standard deviation within every meter of depth, and secondly, generating a fifth-order polynomial fit for the vertical profiles of means and standard deviations using `numpy.polyfit` for each season. The coefficients are listed below in Table S16.

## S1.2 Supplementary Tables

**Table S1:** Summary of the ECOSMO II parameter set used for this study. Values in square brackets indicate different configurations for the respective experiments. This means, the first value is for the Redfield-based model, the second for the model with preferential remineralization only, the third with both preferential remineralization and extracellular release and the fourth with extracellular release only. For the variable stoichiometry ECOSMO II model description, see below in section S2 of the Supplementary Material.

Definition	Abbr.	Value	Unit
Maximum growth rate for $P_2$ (diatoms)	$\sigma_{P_2}$	1.30	[ $d^{-1}$ ]
Maximum growth rate for $P_1$ (flagellates)	$\sigma_{P_1}$	1.10	[ $d^{-1}$ ]
Photosynthesis efficiency	$\alpha$	0.01	[ $m^2 W^{-1}$ ]
Phytoplankton self-shading	$\kappa_{\text{phyto}}$	0.03	[ $m^2 (mmolC)^{-1}$ ]
Particulate organic matter (POM) self-shading	$\kappa_{\text{POM}}$	0.20	[ $m^2 (mmolC)^{-1}$ ]
Dissolved organic matter (DOM) self-shading	$\kappa_{\text{DOM}}$	0.29	[ $m^2 (mmolC)^{-1}$ ]
Water background light extinction coefficient	$\kappa_W$	0.03	[ $m^{-1}$ ]
External suspended particulate matter (SPM) light extinction coefficient	$\kappa_{\text{SPM}}$	0.0	[ $mg l^{-1} m^{-1}$ ]
Photosynthetically active radiation (PAR) fraction of incident light	par_fraction	0.6	-
Ammonium ( $\text{NH}_4$ ) half saturation const.	$r_{\text{NH}_4}$	0.20	[ $mmolN m^{-3}$ ]
Nitrate ( $\text{NO}_3$ ) half saturation const.	$r_{\text{NO}_3}$	0.5	[ $mmolN m^{-3}$ ]
Ammonium ( $\text{NH}_4$ ) inhibition parameter	$\Psi$	3.0	[ $m^3 (mmolN)^{-1}$ ]
Diatom mortality rate	$m_{P_2}$	0.04	[ $d^{-1}$ ]
Flagellate mortality rate	$m_{P_1}$	0.08	[ $d^{-1}$ ]
Grazing rate of meso-zooplankton on phytoplankton	$\sigma_{Z_2,P}$	0.8	[ $d^{-1}$ ]
Grazing rate of micro-zooplankton on phytoplankton	$\sigma_{Z_1,P}$	1.0	[ $d^{-1}$ ]
Grazing rate of meso-zooplankton on micro-zooplankton	$\sigma_{Z_2,Z_1}$	0.5	[ $d^{-1}$ ]
Zooplankton half saturation constant	$r_Z$	0.5	[ $mmolC m^{-3}$ ]
Meso-zooplankton mortality rate	$m_{Z_2}$	0.1	[ $d^{-1}$ ]
Micro-zooplankton mortality rate	$m_{Z_1}$	0.2	[ $d^{-1}$ ]
Meso-zooplankton excretion rate	$\mu_{Z_2}$	0.06	[ $d^{-1}$ ]
Micro-zooplankton excretion rate	$\mu_{Z_1}$	0.08	[ $d^{-1}$ ]
Meso-zooplankton assimilation efficiency on plankton	$\gamma_{Z_2,P}$	0.75	-
Micro-zooplankton assimilation efficiency on plankton	$\gamma_{Z_1,P}$	0.75	-
Zooplankton assimilation efficiency on POM	$\gamma_{Z,POM}$	0.75	-
POC remineralization rate	$\varepsilon_{POC}$	0.003	[ $d^{-1}$ ]

POM sinking rate	$w_{POM}$	5.0	[m d <sup>-1</sup> ]
Phosphate (PO <sub>4</sub> ) half saturation const.	$r_{PO_4}$	0.05	[mmolP m <sup>-3</sup> ]
Silicate (SiO <sub>2</sub> ) half saturation const.	$r_{Si}$	0.5	[mmolSi m <sup>-3</sup> ]
Silicate (SiO <sub>2</sub> ) remineralization rate	$\varepsilon_{Si}$	0.015	[d <sup>-1</sup> ]
Maximum growth rate of cyanobacteria	$\sigma_{P_3}$	1.0	[d <sup>-1</sup> ]
Cyanobacteria temperature control	$T_{ctrl,P_3}$	1.0	[°C <sup>-1</sup> ]
Cyanobacteria reference temperature	$T_{ref,P_3}$	0.0	[°C]
Cyanobacteria maximum grazing rate	$\beta_{P_3}$	0.3	[d <sup>-1</sup> ]
Cyanobacteria mortality rate	$m_{P_3}$	0.08	[d <sup>-1</sup> ]
Critical bottom shear stress for resuspension	$\tau_{crit}$	0.007	[N m <sup>-2</sup> ]
Resuspension rate for $\tau > \tau_{crit}$	$\lambda_{res}$	25.0	[d <sup>-1</sup> ]
Sedimentation rate for $\tau \leq \tau_{crit}$	$\lambda_{dep}$	3.5	[m d <sup>-1</sup> ]
Burial rate	$\delta_{bur}$	0.00001	[d <sup>-1</sup> ]
Sediment base remineralization rate	$\varepsilon_{Sed}$	0.001	[d <sup>-1</sup> ]
Temperature control of denitrification	$T_{ref,denit}$	0.15	[°C <sup>-1</sup> ]
Sed. PIP release parameter p1	RelSEDp1	0.15	-
Sed. PIP release parameter p2	RelSEDp2	0.10	-
Sed. remineralization rate Si	$\varepsilon_{Sed3}$	0.0002	[d <sup>-1</sup> ]
Biogenic opal (SiO <sub>2</sub> · 2H <sub>2</sub> O) sinking rate	$w_{Opal}$	5.0	[m d <sup>-1</sup> ]
Cyanobacteria sinking rate	$w_{P_3}$	-1.0	[m d <sup>-1</sup> ]
Diatom sinking rate	$w_{P_2}$	0.0	[m d <sup>-1</sup> ]
Grazing preference of micro-zooplankton on flagellates	$a_{Z_1,P_1}$	0.7	-
Grazing preference of micro-zooplankton on diatoms	$a_{Z_1,P_2}$	0.25	-
Grazing preference of micro-zooplankton on particulate organic matter	$a_{Z_1,POM}$	0.1	-
Grazing preference of micro-zooplankton on cyanobacteria	$a_{Z_1,P_3}$	0.3	-
Grazing preference of meso-zooplankton on flagellates	$a_{Z_2,P_1}$	0.1	-
Grazing preference of meso-zooplankton on diatoms	$a_{Z_2,P_2}$	0.85	-
Grazing preference of meso-zooplankton on micro-zooplankton	$a_{Z_2,Z_1}$	0.15	-
Grazing preference of meso-zooplankton on particulate organic matter	$a_{Z_2,POM}$	0.1	-
Grazing preference of meso-zooplankton on cyanobacteria	$a_{Z_2,P_3}$	0.3	-
Fraction of dissolved organic matter from new detrital matter	$a_{DOM}$	0.4	-

Fraction of particulate organic matter from new detrital matter	$a_{\text{POM}} = (1 - a_{\text{DOM}})$	0.6	-
Surface deposition of nitrate (here provided from monthly observations instead)	Surf <sub>NO<sub>3</sub></sub>	0.08	[mmolN m <sup>-2</sup> d <sup>-1</sup> ]
Surface deposition of ammonium (here provided from monthly observations instead)	Surf <sub>NH<sub>4</sub></sub>	0.05	[mmolN m <sup>-2</sup> d <sup>-1</sup> ]
Surface deposition of phosphate	Surf <sub>PO<sub>4</sub></sub>	0.0	[mmolP m <sup>-2</sup> d <sup>-1</sup> ]
Surface deposition of silicate	Surf <sub>SiO<sub>2</sub></sub>	0.0	[mmolSi m <sup>-2</sup> d <sup>-1</sup> ]
Minimum daily radiation for cyanobacteria growth	$I_{P_3}$	120	[W m <sup>-2</sup> ]
Minimum daily photosynthetically active radiation for nitrogen fixation	PAR <sub>P<sub>3</sub></sub>	120	[W m <sup>-2</sup> ]
Remineralization ratio of DOC to POC	$\epsilon_{\text{DOC:POC}}$	0.5	-
Remineralization ratio of POC to PON	$\epsilon_{\text{POC:PON}}$	[1, 0.625, 0.7692, 1]	-
Remineralization ratio of POC to POP	$\epsilon_{\text{POC:POP}}$	[1, 0.5, 0.6666, 1]	-
Remineralization ratio of DOC to DON	$\epsilon_{\text{DOC:DON}}$	[1, 0.625, 0.7692, 1]	-
Remineralization ratio of DOC to DOP	$\epsilon_{\text{DOC:DOP}}$	[1, 0.5, 0.6666, 1]	-
Rate of flocculation from DOM to POM	$F_{\text{DOM2POM}}$	[0, 0, 0.02, 0.02]	-
Extracellular release scaling factor	$B_{\text{ER}}$	[0, 0, 0.2, 0.4]	-

**Table S2:** Model percentage biases for all four configurations RS, ER, PR and ER&PR with respect to observations for dissolved inorganic carbon (DIC), total alkalinity (TA), and surface partial pressure of CO<sub>2</sub> (pCO<sub>2</sub>) across different subareas of the northwest European shelf seas. Both DIC and TA observations are from the Global Ocean Data Analysis Project (GLODAP), whereas pCO<sub>2</sub> measurements are from the Surface Ocean CO<sub>2</sub> Atlas (SOCAT).

Model percentage bias [%] compared to co-located observational data from GLODAP, SOCAT and ICES					
Variable	Sub-Region	RS	ER	PR	ER&PR
DIC	NNS	0.661	0.596	0.630	0.610
	CNS	1.105	0.947	1.025	0.967
	SNS	1.254	1.149	1.100	1.101
	NT	0.870	0.975	0.871	0.916
	SK	1.115	1.319	1.140	1.195
TA	NNS	0.544	0.542	0.542	0.541
	CNS	0.884	0.891	0.856	0.869
	SNS	0.872	0.882	0.850	0.866
	NT	0.666	0.664	0.660	0.660
	SK	0.917	0.909	0.914	0.912
pCO <sub>2</sub>	NNS	4.492	4.337	4.313	4.100
	CNS	7.993	6.341	6.978	6.297
	SNS	15.119	13.441	14.002	13.379
	NT	18.701	16.709	17.723	16.700
	SK	24.801	29.812	24.277	27.552
	EC	11.591	10.076	11.118	10.520
	SWC	7.158	9.202	7.167	7.608
	AS	16.642	13.367	14.731	13.718

**Table S3:** Literature compilation of observational data on concentrations of bulk dissolved organic carbon (DOC), nitrogen (DON), and phosphorus (DOP), including both the (semi-) labile and refractory fractions of dissolved organic matter (DOM). Individual numbers without parentheses represent averages over regions or a series of measurements, whereas values in parentheses show ranges between individual measurements or sub-regions. Ranges of concentrations with a double-asterisk represent estimates from figures in the respective references. For the data from Lønborg et al. (2024), we report the median along with the 25<sup>th</sup> and 75<sup>th</sup> percentiles, as these better represent the distribution of the large dataset, avoiding the influence of outliers on the mean and range.

Location	Sub-Region or Focus	Bulk DOM Concentrations			Source
		DOC [ $\mu\text{M}$ ]	DON [ $\mu\text{M}$ ]	DOP [ $\mu\text{M}$ ]	
Global Ocean	Surface Ocean Biogeochemical Regions	65.8 (52.4–73.5)	4.5 (3.7–5.3)	0.17 (0.11–0.27)	(Liang et al., 2023)
	Full Water Column	(46.2–65.3)	(2.1–4.5)	(0.04–0.19)	(Letscher et al., 2015; Letscher and Moore, 2015)
	Coastal Ocean	(50–60)	(4.5–45)	(0.08–0.50)	(Lønborg and Álvarez-Salgado, 2012)
	Coastal Ocean	103 (77–228)	8.0 (5.5–15.8)	0.18 (0.11–0.30)	(Lønborg et al., 2024)
	Shelf, Slope and Open Ocean (surface only 0–100m)	(30–160)**	(1–11)**	(0.00–0.45)**	(Hopkinson and Vallino, 2005)
Atlantic Ocean	Georges Bank (Surface Ocean)	65–92	5	0.17	(Hopkinson et al., 1997)
	Georges Bank (Deep Waters)	50	3	0.02	(Hopkinson et al., 1997)
	Middle Atlantic Bight (Surface Ocean)	125 (81–201)	10.2 (7.1–14.3)	0.30 (0.14–0.42)	(Hopkinson et al., 2002)
	Middle Atlantic Bight (Deep Slope Waters)	46.7	2.76	0.03	(Hopkinson et al., 2002)
	Northeast Atlantic (Surface Waters)	(61–83)	(4.2–6.1)	(0.07–0.14)	(Aminot and Kéroutil, 2004)
	Northeast Atlantic (Deep Waters)	(41–55)	(2.6–4.0)	(0.01–0.08)	(Aminot and Kéroutil, 2004)
Pacific Ocean	Eastern North Pacific	(35–72)	(1.5–4.5)	(0.013–0.229)	(Loh and Bauer, 2000)
	North Pacific Subtropical Gyre	(63–105)	(3.7–6.2)	(0.10–0.27)	(Church et al., 2002)
Southern Ocean	-	(39–53)	(2.5–5.2)	(0.061–0.225)	(Loh and Bauer, 2000)
Mediterranean Sea	Southern Adriatic Basin (Surface)	(49–79)	(2.3–7.2)	(0.02–0.08)	(Santinelli et al., 2012)
	Southern Adriatic Basin (Intermediate Waters)	(45–54)	(1.8–5.3)	(0.02–0.06)	(Santinelli et al., 2012)
	Southern Adriatic Basin (Deep Waters)	(47–60)	(2.9–6.2)	(0.02–0.08)	(Santinelli et al., 2012)
	Northwestern Mediterranean	(44–95)	(2.8–6.2)	-	(Doval et al., 1999)
	Northwestern Mediterranean	(40–120)**	(0–6)**	(0.0–0.4)**	(Lucea et al., 2003)
	Northwestern Mediterranean (Surface Waters)	(67–69)	(4.0–4.2)	(0.08–0.08)	(Aminot and Kéroutil, 2004)

	Northwestern Mediterranean (Deep Waters)	(46–48)	(2.7–3.0)	(0.03–0.04)	(Aminot and Kéroutil, 2004)
	Northwestern Mediterranean	(80–100)	(4.5–5.5)	(0.06–0.10)	(Raimbault et al., 1999)
	Western Basin	(37.6–69.4)	(2.5–5.5)	(0–0.09)	(Pujo-Pay et al., 2011)
	Eastern Basin	(37.5–72.4)	(2.1–6.3)	(0–0.10)	(Pujo-Pay et al., 2011)
East China Sea	-	(60–120)	(6–9.6)	(0.05–0.25)	(Hung et al., 2003)
South China Sea	Northern Parts	(43–132)	-	-	(Hung et al., 2007)
northwest European shelf seas	Norwegian Coastal Waters	-	(8–11.5)**	-	(Frigstad et al., 2013)
	Celtic Sea	(65–70)	(3.9–6)	(0.19–0.35)	(Davis et al., 2019)
	North Sea	46.9–107.5 (32.7–224.8)	5.2–9.0 (2.8–13.7)	-	(Chaichana et al., 2017, 2019)
	northern North Sea (Surface)	60.7–73.8 (32.7–104.2)	5.3–6.6 (3.0–8.7)	-	(Chaichana et al., 2017, 2019)
	northern North Sea (Bottom)	46.9–73.8 (36.8–120.1)	5.2–5.9 (1.0–11.7)	-	(Chaichana et al., 2017, 2019)
	southern North Sea	65.5–97.5 (36.3–224.8)	5.3–9.0 (2.8–13.7)	-	(Chaichana et al., 2017, 2019)
	central North Sea	(68–318)	(2–11)**	-	(Suratman et al., 2009)
	North Sea	108.7 (61.7–185.0)	6.6 (3.5–16.4)	0.26 (0.13–0.46)	(Painter et al., 2018)
Baltic Sea	Bothnian Sea	466	-	-	(Rowe et al., 2018)
	Bothnian Bay	416	-	-	(Rowe et al., 2018)
	Gulf of Finland	(290–724)	(8.6–38.5)	(0.06–0.80)	(Hoikkala et al., 2012, 2015)
	Gulf of Bothnia	(241–520)	(7.8–14.8)	(0.12–0.18)	(Hoikkala et al., 2015)
	Gulf of Riga	(400–1230)	(10–38)	(0.5–0.9)	(Hoikkala et al., 2015)
	Baltic Proper	(259–708)	(10.2–203)	-	(Hoikkala et al., 2015; Rowe et al., 2018)
	Estuaries	(318.41–736.74)	(14.14–45.22)	(0.14–0.38)	(Voss et al., 2021)
	Southwestern Baltic Sea (Heiligendamm)	290	17.2	-	(Osterholz et al., 2021)
	Gotland Basin	-	-	(0.20–0.29)	(Nausch et al., 2008)

**Table S4:** Literature compilation of observational data on concentrations of biodegradable or (semi-)labile dissolved organic carbon (LDOC), nitrogen (LDON), and phosphorus (LDOP). Individual numbers or ranges (e.g., between sub-regions or different years) without parentheses represent averages over regions or a series of measurements whereas values in parentheses show ranges between individual measurements. The given percentage indicates the fraction of labile dissolved organic carbon, nitrogen, and phosphorus in relation to the bulk pool.

Location	Sub-Region or Focus	Biodegradable or (Semi-)Labile DOM Concentrations			Source
		LDOC [ $\mu M$ ]	LDON [ $\mu M$ ]	LDOP [ $\mu M$ ]	
Global Ocean	Surface Ocean Biogeochemical Regions	25.0 (10.5–29.1)	2.8 (1.9–3.5)	0.14 (0.06–0.22)	(Liang et al., 2023)
	Shelf, Slope and Open Ocean	(15–80)	-	-	(Hopkinson and Vallino, 2005)
	Coastal Ocean	(1–199) (2–51%)	(0.6–15.2) (10–65%)	(0.04–0.33) (30–96%)	(Lønborg and Álvarez-Salgado, 2012)
Atlantic Ocean	Northeast Atlantic	(16.0–16.3) (26–27%)	(1.5–1.6) (34–36%)	(0.04–0.10) (60–78%)	(Aminot and Kérouel, 2004)
Mediterranean Sea	Northwestern Mediterranean	23.3 34%	1.2 30%	0.04 60%	(Aminot and Kérouel, 2004)
Baltic Sea	Open Sea Only	(0–82) (0–17%)	(0–6.5) (0–41%)	(0.01–0.34) (8–65%)	(Hoikkala et al., 2012, 2015)

**Table S5:** Literature compilation of observational data on concentrations of refractory or recalcitrant dissolved organic carbon (RDOC), nitrogen (RDON), and phosphorus (RDOP). Individual numbers or ranges (e.g., between sub-regions or different years) without parentheses represent averages over regions or a series of measurements whereas values in parentheses show ranges between individual measurements.

Location	Sub-Region or Focus	Refractory or Recalcitrant DOM Concentrations			Source
		RDOC [ $\mu M$ ]	RDON [ $\mu M$ ]	RDOP [ $\mu M$ ]	
Global Ocean	Surface Ocean	46 (45–49)	2.7 (2.5–2.8)	-	(Liang et al., 2023)
	Deep Ocean	42	3.0	0.05	(Liang et al., 2023)
	Surface Ocean	42	-	-	(Hopkinson and Vallino, 2005)
	Deep Ocean	34	-	-	(Hopkinson and Vallino, 2005)
	Deep Ocean	(33.8–48.1)	-	-	(Hansell and Carlson, 1998)
Atlantic and Mediterranean	NE Atlantic and NW Mediterranean	44.9 (43.8–45.9)	2.85 (2.73–3.00)	0.029 (0.023–0.034)	(Aminot and Kérouel, 2004)

**Table S6:** Literature compilation of observational data on concentrations of particulate organic carbon (POC), nitrogen (PON), and phosphorus (POP). Individual numbers or ranges (e.g., between sub-regions or different years) without parentheses represent averages over regions or a series of measurements whereas values in parentheses show ranges between individual measurements. Ranges of concentrations with a double-asterisk represent estimates from figures in the respective references. Strong outliers in the measurement referenced as “Patch” were excluded from (Nausch et al., 2008).

Location	Sub-Region or Focus	POM Concentrations			Source
		POC [ $\mu M$ ]	PON [ $\mu M$ ]	POP [ $nM$ ]	
Global Ocean	Surface Ocean Biogeochemical Regions	6.4 (2.3–17.2)	0.83 (0.32–2.2)	40 (10–170)	(Liang et al., 2023; Martiny et al., 2014; Tanioka et al., 2022)
Pacific Ocean	Eastern North Pacific	(0.09–5.76)	(0.012–0.917)	(0.45–37.32)	(Loh and Bauer, 2000)
Southern Ocean	South of the Tasman Sea	(0.05–3.48)	(0.004–0.490)	(0.25–13.48)	(Loh and Bauer, 2000)
Mediterranean Sea	NW Mediterranean	(0.9–14.9)	(0.1–1.7)	-	(Doval et al., 1999)
	NW Mediterranean	(4–15)**	(0.2–0.7)**	(0–55)**	(Lucea et al., 2003)
	Western Basin	(0.74–8.70)	(0.01–0.87)	(1–45)	(Pujo-Pay et al., 2011)
	Eastern Basin	(0.70–5.41)	(0.01–0.66)	(1–30)	(Pujo-Pay et al., 2011)
South China Sea	Northern Parts	(1.1–13)	-	-	(Hung et al., 2007)
northwest European shelf seas	Hebrides Shelf	(4.73–6.74)	(0.37–0.76)	(1–10)	(Painter et al., 2017)
	Norwegian Coastal Waters	(6–14)**	(0.8–2.5)**	(6–14)**	(Frigstad et al., 2013)
	Celtic Sea	(2–15)**	(0.2–3)**	(1–13)**	(Davis et al., 2019)
	North Sea	7.3–16.0 (1.1–43.8)	1.5–2.2 (0.3–5.9)	-	(Chaichana et al., 2017, 2019)
	northern North Sea (Surface)	10.5 (2.7–21.8)	2.0 (0.6–2.9)	-	(Chaichana et al., 2017, 2019)
	northern North Sea (Bottom)	7.3 (1.1–16.2)	1.5 (0.3–2.7)	-	(Chaichana et al., 2017, 2019)
	southern North Sea	16.0 (5.8–43.8)	2.2 (0.6–5.9)	-	(Chaichana et al., 2017, 2019)
	central North Sea	(1.9–38.4)	(0.2–5.8)**	-	(Suratman et al., 2009)
Baltic Sea	Estuaries	(29.8–388)	-	-	(Voss et al., 2021)
	Gotland and Gdansk Deep	(8.3–79.9)	(0.7–11.4)	-	(Winogradow et al., 2019)
	SW Baltic Sea (Heiligendamm)	33	4.8	-	(Osterholz et al., 2021)
	Gotland Basin	(27.98–93.92)	(3.88–13.42)	(140–390)	(Nausch et al., 2008)

**Table S7:** Literature compilation of observational data on elemental ratios of carbon, nitrogen, and phosphorus in bulk dissolved organic matter (DOM). Individual numbers or ranges (e.g., between sub-regions or different years) without parentheses represent averages over regions or a series of measurements whereas values in parentheses show ranges between individual measurements. A single asterisk indicates implicit estimates of individual C:N, C:P or N:P ratios from provided ranges of C:N:P ratios where they were not provided explicitly. Ranges of values with a double-asterisk represent estimates from figures in the respective references. For the data from Lønborg et al. (2024), we report the median along with the 25<sup>th</sup> and 75<sup>th</sup> percentiles, as these better represent the distribution of the large dataset, avoiding the influence of outliers on the mean and range.

Location	Sub-region or focus	Bulk DOM stoichiometry			Source
		DOC:DON	DOC:DOP	DON:DOP	
Global ocean	Global surface ocean (biogeochemical regions)	14.6 (13.0–16.1)	387 (251–638)	26 (17–44)	(Liang et al., 2023)
	Full water column	17*	810	48	(Letscher et al., 2015; Letscher and Moore, 2015)
	Coastal ocean	9*	1164	123	(Lønborg and Álvarez-Salgado, 2012)
	Coastal ocean	14 (11–18)	583 (401–1034)	47 (30–78)	(Lønborg et al., 2024)
	Shelf, slope, and open ocean	14*	778	54	(Hopkinson and Vallino, 2005)
	Shelf, slope, and open ocean (surface only 0–100m)	14	374	27	(Hopkinson and Vallino, 2005)
Atlantic Ocean	Georges Bank (Surface Ocean)	(11–15)	(400–800)	(24–55)	(Hopkinson et al., 1997)
	Geroges Bank (Deep Waters)	(14–20)	(700–2500)	(40–140)	(Hopkinson et al., 1997)
	Middle Atlantic Bight (Surface Ocean)	12 (9–14)*	431 (290–1101)	36 (25.8–86.7)	(Hopkinson et al., 2002)
	Middle Atlantic Bight (Deep Slope Waters)	13 (12–14)*	2700 (986–4404)	215 (70–360)	(Hopkinson et al., 2002)
	NE Atlantic (Surface Waters)	(13.1–14.3)	(440–850)	(31–62)	(Aminot and Kéroutil, 2004)
	NE Atlantic (Deep Waters)	(12.6–16.4)	(640–3100)	(45–200)	(Aminot and Kéroutil, 2004)
Pacific Ocean	Eastern North Pacific	(13–30)	(277–537)	(13–34)	(Loh and Bauer, 2000)
	North Pacific Subtropical Gyre	(14.8–16.4)	(390–483)	(24.0–31.4)	(Church et al., 2002)
Southern Ocean	South of the Tasman Sea	(9–18)	(229–682)	(12–49)	(Loh and Bauer, 2000)
Mediterranean Sea	Southern Adriatic Basin (Surface)	(14–16)	(1189–1411)	(86–88)	(Santinelli et al., 2012)
	Southern Adriatic Basin (Intermediate Waters)	(13–14)	(1107–1279)	(83–97)	(Santinelli et al., 2012)
	Southern Adriatic Basin (Deep Waters)	(11–15)	(993–1693)	(85–108)	(Santinelli et al., 2012)
	NW Mediterranean	15.5	-	-	(Doval et al., 1999)
	NW Mediterranean	(30–60)*	(1510–1984)	(25–66)	(Lucea et al., 2003)

	NW Mediterranean (Surface Waters)	(16.7–16.9)	(920–970)	(55–57)	(Aminot and Kéroutil, 2004)
	NW Mediterranean (Deep Waters)	(15.1–17.2)	(1100–1800)	(64–106)	(Aminot and Kéroutil, 2004)
	Western Basin	12.1	1941	162.7	(Pujo-Pay et al., 2011)
	Eastern Basin	13.0	2055	160.8	(Pujo-Pay et al., 2011)
East China Sea	-	(8.9–15.3)	(200–853)	(19–83.6)	(Hung et al., 2003)
South China Sea	Northern Parts	(11–13)*	(322–510)	(29–39)	(Hung et al., 2007)
Sea of Japan (East Sea)	-	17*	374	22	(Kim and Kim, 2013)
northwest European shelf seas	Norwegian Coastal Waters	-	-	(59.8–73.6)	(Frigstad et al., 2013)
	Celtic Sea	(12–17)*	(281–416)	(17–33)	(Davis et al., 2014)
	Celtic Sea	(11.0–17.4)	(147–377)	(11.7–31.7)	(Davis et al., 2019)
	North Sea	(5.9–36.5)	-	-	(Chaichana et al., 2017, 2019)
	central North Sea	(9.5–67.4)	-	-	(Suratman et al., 2009)
	North Sea	(10–25)**	(200–900)**	(15–75)**	(Painter et al., 2018)
Baltic Sea	Baltic Proper	31.6	527.0	16.6	(Rowe et al., 2018)
	Bothnian Sea	21.3	402.6	18.9	(Rowe et al., 2018)
	Bothnian Bay	23.1	780.7	33.8	(Rowe et al., 2018)
	Gulf of Finland	(10–54)	-	(25–419)	(Hoikkala et al., 2012, 2015)
	Gulf of Bothnia	(25–28)	-	100	(Hoikkala et al., 2015)
	Gulf of Riga	-	-	(20–60)	(Hoikkala et al., 2015)
	Baltic Proper	(17–26)	-	(20–30)	(Hoikkala et al., 2015)
	Estuaries	(16–23)*	(1199–3714)	(52–221)	(Voss et al., 2021)
	Rivers	31*	2790	91	(Stepanauskas et al., 2002)
	Southwestern Baltic Sea (Heiligendamm)	(12.5–20)**	-	-	(Osterholz et al., 2021)

**Table S8:** Literature compilation of observational data on elemental ratios of carbon, nitrogen, and phosphorus in biodegradable or (semi-)labile dissolved organic matter (LDOM). Individual numbers or ranges (e.g., between sub-regions or different years) without parentheses represent averages over regions or a series of measurements whereas values in parentheses show ranges between individual measurements. A single asterisk indicates implicit estimates from provided ranges of C:N:P ratios where they were not provided explicitly.

Location	Sub-region or focus	Biodegradable or (semi-)labile DOM stoichiometry			Source
		LDOC:LDON	LDOC:LDOP	LDON:LDOP	
Global ocean	Global surface ocean (biogeochemical regions)	8.9 (5.4–12.0)	179 (83–414)	20 (15–49)	(Liang et al., 2023)
	Coastal ocean	(8–9)*	(197–216)	(24–25)	(Lønborg and Álvarez-Salgado, 2012)
	Shelf, slope, and open ocean	10.7 (8.7–14.1)	199 (154–245)	20 (15.6–25)	(Hopkinson and Vallino, 2005)
Atlantic	NE Atlantic	(10.1–10.7)	(159–380)	(14.8–38)	(Aminot and Kéruel, 2004)
	Middle Atlantic Bight	(10.0–14.1)	(193–203)	(15.6–20.2)	(Hopkinson and Vallino, 2005)
	Georges Bank	9.8	245	25	(Hopkinson and Vallino, 2005)
Pacific Ocean	Hawaiian Ocean	8.7	154	17.8	(Hopkinson and Vallino, 2005)
Mediterranean Sea	NW Mediterranean	19.2	530	28	(Aminot and Kéruel, 2004)
Baltic Sea	Gulf of Finland	(0.8–11.7)	-	-	(Hoikkala et al., 2012, 2015)

**Table S9:** Literature compilation of observational data on elemental ratios of carbon, nitrogen, and phosphorus in refractory or recalcitrant dissolved organic matter (RDOM). Individual numbers or ranges (e.g., between sub-regions or different years) without parentheses represent averages over regions or a series of measurements whereas values in parentheses show ranges between individual measurements. A single asterisk indicates implicit estimates from provided ranges of C:N:P ratios where they were not provided explicitly.

Location	Refractory or recalcitrant DOM stoichiometry			Source
	RDOC:RDON	RDOC:RDOP	RDON:RDOP	
Global ocean	17.0 (16.5–18.1)	1373 (900–2300)	82 (50–140)	(Liang et al., 2023)
Coastal ocean	18*	2835	159	(Lønborg and Álvarez-Salgado, 2012)
Shelf, slope, and open ocean	17*	3511	202	(Hopkinson and Vallino, 2005)
NE Atlantic and NW Mediterranean	15.7	1570	10	(Aminot and Kérouel, 2004)

**Table S10:** Literature compilation of observational data on elemental ratios of carbon, nitrogen, and phosphorus in particulate organic matter (POM). Individual numbers represent averages over regions or a series of measurements whereas values in parentheses show ranges between sub-regions or measurements. A single asterisk indicates implicit estimates from provided ranges of C:N:P ratios where they were not provided as individual ratios explicitly. Ranges of values with a double-asterisk represent estimates from figures in the respective references.

Location	Sub-region or focus	POM stoichiometry			Source
		POC:PON	POC:POP	PON:POP	
Global Ocean	Surface ocean	7.7 (6.1–9.2)	160 (73–295)	21 (10–37)	(Liang et al., 2023; Martiny et al., 2014; Tanioka et al., 2022)
	-	6.6	163	22	(Martiny et al., 2014)
	Surface layer (50m)	-	146	-	(Tanioka et al., 2021)
	Twilight zone (100–1000m)	-	294 (83–500)	-	(Tanioka et al., 2021)
	Bermuda Atlantic	6 (1–19)	210 (45–532)	36 (7–140)	(Singh et al., 2015)
Pacific Ocean	Eastern North Pacific	(6–10)	(117–630)	(12–74)	(Loh and Bauer, 2000)
Southern Ocean	-	(4–14)	(59–336)	(6–46)	(Loh and Bauer, 2000)
Mediterranean Sea	NW Mediterranean	8.6	-	-	(Doval et al., 1999)
	NW Mediterranean	(14–19)*	(220–426)	(15–22)	(Lucea et al., 2003)
	Western Basin	13.3	256	19.8	(Pujo-Pay et al., 2011)
	Eastern Basin	14.0	235	18.8	(Pujo-Pay et al., 2011)
South China Sea	Northern Parts	(8–12)*	(148–502)	(18–42)	(Hung et al., 2007)
northwest European shelf seas	Hebrides Shelf	(8.26–13.67)	(142.4–259.97)	(16.4–26.32)	(Painter et al., 2017)
	Norwegian Coastal Waters	(7.1–7.4)	(110.8–125.2)	(14.6–17.6)	(Frigstad et al., 2013)
	Celtic Sea	(5–6)*	(63–223)	(10–38)	(Davis et al., 2014)
	Celtic Sea	(4.3–11.6)	(144–283)	(24–47)	(Davis et al., 2019)
	North Sea	(0.7–16.8)	-	-	(Chaichana et al., 2017, 2019)
	central North Sea	(2.5–34.9)	-	-	(Suratman et al., 2009)
Baltic Sea	Estuaries	6*	253	39	(Voss et al., 2021)
	Gotland and Gdansk Deep	(5.8–10.8)	-	-	(Winogradow et al., 2019)
	SW Baltic Sea (Heiligenhafen)	(2.5–11)**	-	-	(Osterholz et al., 2021)

**Table S11:** Annual vertically- and subarea-integrated carbon fixation averaged over the simulation period 2000–2010 for all four model configurations: Redfield Stoichiometry (RS), Extracellular Release (ER), Preferential Remineralization (PR), and the combined configuration (ER&PR). For each configuration, the mean is provided both area-integrated and per area. The variable stoichiometry configurations also include the per area difference with respect to the RS configuration.

Annual vertically- and subarea-integrated carbon fixation averaged over 2000–2010												
Subarea	RS		ER			PR			ER&PR			
	Total [TmolC yr <sup>-1</sup> ]	Per Area [molC m <sup>-2</sup> yr <sup>-1</sup> ]	Total [TmolC yr <sup>-1</sup> ]	Per Area [molC m <sup>-2</sup> yr <sup>-1</sup> ]	Difference [molC m <sup>-2</sup> yr <sup>-1</sup> ]	Total [TmolC yr <sup>-1</sup> ]	Per Area [molC m <sup>-2</sup> yr <sup>-1</sup> ]	Difference [molC m <sup>-2</sup> yr <sup>-1</sup> ]	Total [TmolC yr <sup>-1</sup> ]	Per Area [molC m <sup>-2</sup> yr <sup>-1</sup> ]	Difference [molC m <sup>-2</sup> yr <sup>-1</sup> ]	
Entire NWES	9.708	7.909	14.790	12.049	+4.141	10.593	8.630	+0.721	12.786	10.416	+2.508	
Entire North Sea	4.473	7.413	6.923	11.474	+4.061	4.922	8.158	+0.745	5.994	9.935	+2.522	
northern North Sea	0.598	7.591	0.907	11.515	+3.924	0.632	8.033	+0.441	0.775	9.849	+2.257	
central North Sea	1.739	7.155	2.870	11.807	+4.652	1.919	7.896	+0.741	2.434	10.013	+2.858	
southern North Sea	1.518	7.446	2.180	10.694	+3.248	1.696	8.321	+0.874	1.962	9.621	+2.175	
Norwegian Trench	0.618	7.951	0.966	12.437	+4.486	0.674	8.682	+0.731	0.823	10.600	+2.649	
English Channel	0.676	8.210	0.952	11.562	+3.352	0.737	8.947	+0.737	0.850	10.323	+2.113	
Skagerrak Kattegat	0.471	6.056	0.747	9.601	+3.546	0.535	6.875	+0.820	0.644	8.275	+2.220	
NE Celtic Sea	0.973	9.078	1.448	13.510	+4.432	1.045	9.746	+0.668	1.252	11.684	+2.605	
SW Celtic Sea	0.832	9.101	1.320	14.439	+5.338	0.886	9.694	+0.594	1.105	12.097	+2.996	
Irish Sea	0.408	8.547	0.533	11.175	+2.627	0.429	8.980	+0.432	0.479	10.035	+1.487	
Inner Seas (Scotland)	0.382	8.630	0.541	12.212	+3.582	0.405	9.140	+0.509	0.474	10.705	+2.075	
Armorican Shelf	0.603	8.626	0.992	14.190	+5.564	0.685	9.807	+1.181	0.838	11.987	+3.361	
Hebrides Shelf	0.302	8.491	0.453	12.749	+4.257	0.321	9.025	+0.534	0.391	10.990	+2.499	
Malin Shelf	0.190	8.960	0.282	13.264	+4.304	0.199	9.387	+0.427	0.241	11.360	+2.400	
West Irish Shelf	0.401	8.507	0.603	12.815	+4.308	0.432	9.175	+0.668	0.520	11.052	+2.545	

**Table S12:** Annual vertically- and subarea-integrated pelagic carbon remineralization averaged over the simulation period 2000–2010 for all four model configurations: Redfield Stoichiometry (RS), Extracellular Release (ER), Preferential Remineralization (PR), and the combined configuration (ER&PR). For each configuration, the mean is provided both area-integrated and per area. The variable stoichiometry configurations also include the per area difference with respect to the RS configuration.

Annual vertically- and subarea-integrated pelagic carbon remineralization averaged over 2000–2010											
Subarea	RS		ER			PR			ER&PR		
	Total [TmolC yr <sup>-1</sup> ]	Per Area [molC m <sup>-2</sup> yr <sup>-1</sup> ]	Total [TmolC yr <sup>-1</sup> ]	Per Area [molC m <sup>-2</sup> yr <sup>-1</sup> ]	Difference [molC m <sup>-2</sup> yr <sup>-1</sup> ]	Total [TmolC yr <sup>-1</sup> ]	Per Area [molC m <sup>-2</sup> yr <sup>-1</sup> ]	Difference [molC m <sup>-2</sup> yr <sup>-1</sup> ]	Total [TmolC yr <sup>-1</sup> ]	Per Area [molC m <sup>-2</sup> yr <sup>-1</sup> ]	Difference [molC m <sup>-2</sup> yr <sup>-1</sup> ]
Entire NWES	9.635	7.849	14.908	12.145	+4.296	10.507	8.560	+0.710	12.834	10.455	+2.606
Entire North Sea	4.528	7.505	7.068	11.715	+4.210	4.971	8.238	+0.733	6.104	10.118	+2.612
northern North Sea	0.571	7.257	0.901	11.443	+4.186	0.606	7.700	+0.443	0.760	9.655	+2.398
central North Sea	1.709	7.032	2.808	11.555	+4.522	1.872	7.703	+0.671	2.379	9.787	+2.755
southern North Sea	1.544	7.574	2.207	10.823	+3.249	1.730	8.487	+0.913	2.000	9.811	+2.237
Norwegian Trench	0.704	9.056	1.152	14.834	+5.777	0.762	9.805	+0.749	0.965	12.425	+3.368
English Channel	0.665	8.077	0.942	11.443	+3.366	0.727	8.833	+0.756	0.840	10.197	+2.121
Skagerrak Kattegat	0.416	5.341	0.731	9.394	+4.053	0.479	6.156	+0.815	0.619	7.948	+2.608
NE Celtic Sea	0.975	9.094	1.449	13.525	+4.430	1.051	9.804	+0.710	1.254	11.705	+2.611
SW Celtic Sea	0.843	9.227	1.364	14.924	+5.697	0.904	9.889	+0.662	1.142	12.495	+3.268
Irish Sea	0.433	9.062	0.569	11.916	+2.854	0.457	9.574	+0.512	0.513	10.738	+1.676
Inner Seas (Scotland)	0.375	8.460	0.545	12.313	+3.853	0.394	8.889	+0.439	0.472	10.665	+2.205
Armorican Shelf	0.556	7.950	0.935	13.377	+5.427	0.627	8.969	+1.019	0.781	11.170	+3.220
Hebrides Shelf	0.299	8.406	0.461	12.966	+4.560	0.315	8.873	+0.466	0.391	10.991	+2.584
Malin Shelf	0.179	8.400	0.279	13.113	+4.713	0.189	8.898	+0.498	0.233	10.959	+2.559
West Irish Shelf	0.364	7.734	0.564	11.981	+4.246	0.391	8.298	+0.564	0.483	10.252	+2.518

**Table S13:** Annual subarea-integrated benthic carbon remineralization averaged over the simulation period 2000–2010 for all four model configurations: Redfield Stoichiometry (RS), Extracellular Release (ER), Preferential Remineralization (PR), and the combined configuration (ER&PR). For each configuration, the mean is provided both area-integrated and per area. The variable stoichiometry configurations also include the per area difference with respect to the RS configuration.

Annual subarea-integrated benthic carbon remineralization averaged over 2000–2010												
Subarea	RS		ER			PR			ER&PR			
	Total [TmolC yr <sup>-1</sup> ]	Per Area [molC m <sup>-2</sup> yr <sup>-1</sup> ]	Total [TmolC yr <sup>-1</sup> ]	Per Area [molC m <sup>-2</sup> yr <sup>-1</sup> ]	Difference [molC m <sup>-2</sup> yr <sup>-1</sup> ]	Total [TmolC yr <sup>-1</sup> ]	Per Area [molC m <sup>-2</sup> yr <sup>-1</sup> ]	Difference [molC m <sup>-2</sup> yr <sup>-1</sup> ]	Total [TmolC yr <sup>-1</sup> ]	Per Area [molC m <sup>-2</sup> yr <sup>-1</sup> ]	Difference [molC m <sup>-2</sup> yr <sup>-1</sup> ]	
Entire NWES	0.706	0.575	0.845	0.689	+0.114	0.832	0.678	+0.102	0.812	0.662	+0.086	
Entire North Sea	0.369	0.611	0.448	0.743	+0.132	0.442	0.732	+0.120	0.430	0.712	+0.101	
northern North Sea	0.039	0.499	0.042	0.539	+0.040	0.043	0.551	+0.053	0.042	0.534	+0.035	
central North Sea	0.102	0.419	0.122	0.502	+0.082	0.125	0.514	+0.094	0.120	0.492	+0.072	
southern North Sea	0.068	0.332	0.101	0.493	+0.162	0.094	0.459	+0.128	0.093	0.454	+0.123	
Norwegian Trench	0.160	2.061	0.183	2.360	+0.299	0.180	2.312	+0.251	0.176	2.259	+0.198	
English Channel	0.002	0.027	0.003	0.032	+0.005	0.003	0.036	+0.009	0.003	0.034	+0.007	
Skagerrak Kattegat	0.135	1.734	0.175	2.246	+0.512	0.155	1.989	+0.255	0.158	2.029	+0.295	
NE Celtic Sea	0.011	0.105	0.013	0.119	+0.013	0.014	0.130	+0.025	0.013	0.123	+0.018	
SW Celtic Sea	0.008	0.084	0.008	0.085	+0.001	0.008	0.089	+0.005	0.008	0.085	+0.001	
Irish Sea	0.005	0.114	0.007	0.138	+0.023	0.007	0.147	+0.033	0.007	0.140	+0.025	
Inner Seas (Scotland)	0.044	0.982	0.048	1.084	+0.102	0.051	1.157	+0.175	0.049	1.105	+0.123	
Armorican Shelf	0.059	0.847	0.067	0.953	+0.106	0.070	1.007	+0.160	0.067	0.959	+0.112	
Hebrides Shelf	0.018	0.508	0.019	0.538	+0.030	0.020	0.569	+0.061	0.019	0.545	+0.037	
Malin Shelf	0.013	0.612	0.014	0.642	+0.030	0.014	0.681	+0.069	0.014	0.648	+0.036	
West Irish Shelf	0.042	0.889	0.045	0.962	+0.073	0.047	0.997	+0.108	0.045	0.958	+0.069	

**Table S14:** Annual vertically- and subarea-integrated net community production (NCP) averaged over the simulation period 2000–2010 for all four model configurations: Redfield Stoichiometry (RS), Extracellular Release (ER), Preferential Remineralization (PR), and the combined configuration (ER&PR). For each configuration, the mean is provided both area-integrated and per area. The variable stoichiometry configurations also include the per area difference with respect to the RS configuration.

Annual vertically- and subarea-integrated net community production averaged over 2000–2010											
Subarea	RS		ER			PR			ER&PR		
	Total [TmolC yr <sup>-1</sup> ]	Per Area [molC m <sup>-2</sup> yr <sup>-1</sup> ]	Total [TmolC yr <sup>-1</sup> ]	Per Area [molC m <sup>-2</sup> yr <sup>-1</sup> ]	Difference [molC m <sup>-2</sup> yr <sup>-1</sup> ]	Total [TmolC yr <sup>-1</sup> ]	Per Area [molC m <sup>-2</sup> yr <sup>-1</sup> ]	Difference [molC m <sup>-2</sup> yr <sup>-1</sup> ]	Total [TmolC yr <sup>-1</sup> ]	Per Area [molC m <sup>-2</sup> yr <sup>-1</sup> ]	Difference [molC m <sup>-2</sup> yr <sup>-1</sup> ]
Entire NWES	-0.633	-0.516	-0.963	-0.785	-0.269	-0.745	-0.607	-0.092	-0.860	-0.701	-0.185
Entire North Sea	-0.425	-0.704	-0.594	-0.984	-0.280	-0.490	-0.812	-0.108	-0.540	-0.895	-0.191
northern North Sea	-0.013	-0.164	-0.037	-0.467	-0.303	-0.017	-0.219	-0.054	-0.027	-0.340	-0.175
central North Sea	-0.072	-0.297	-0.061	-0.249	+0.048	-0.078	-0.321	-0.024	-0.065	-0.266	+0.031
southern North Sea	-0.094	-0.459	-0.127	-0.623	-0.163	-0.128	-0.626	-0.167	-0.131	-0.644	-0.185
Norwegian Trench	-0.246	-3.166	-0.370	-4.757	-1.591	-0.267	-3.436	-0.270	-0.317	-4.084	-0.918
English Channel	0.009	0.106	0.007	0.088	-0.018	0.006	0.078	-0.028	0.008	0.092	-0.014
Skagerrak Kattegat	-0.079	-1.019	-0.159	-2.039	-1.020	-0.099	-1.270	-0.251	-0.132	-1.702	-0.682
NE Celtic Sea	-0.013	-0.121	-0.014	-0.133	-0.012	-0.020	-0.188	-0.067	-0.015	-0.144	-0.023
SW Celtic Sea	-0.019	-0.210	-0.052	-0.570	-0.360	-0.026	-0.284	-0.074	-0.044	-0.484	-0.274
Irish Sea	-0.030	-0.629	-0.042	-0.879	-0.250	-0.035	-0.741	-0.113	-0.040	-0.843	-0.214
Inner Seas (Scotland)	-0.036	-0.812	-0.053	-1.185	-0.373	-0.041	-0.916	-0.104	-0.047	-1.065	-0.253
Armorican Shelf	-0.012	-0.171	-0.010	-0.139	+0.031	-0.012	-0.168	+0.002	-0.001	-0.142	+0.029
Hebrides Shelf	-0.015	-0.423	-0.027	-0.756	-0.332	-0.015	-0.417	+0.007	-0.019	-0.545	-0.122
Malin Shelf	-0.007	-0.312	-0.014	-0.648	-0.336	-0.008	-0.386	-0.075	-0.011	-0.495	-0.183
West Irish Shelf	-0.005	-0.116	-0.006	-0.127	-0.011	-0.006	-0.121	-0.005	-0.007	-0.158	-0.042

**Table S15:** Annual subarea-integrated air-sea CO<sub>2</sub> flux averaged over the simulation period 2000–2010 for all four model configurations: Redfield Stoichiometry (RS), Extracellular Release (ER), Preferential Remineralization (PR), and the combined configuration (ER&PR). For each configuration, the mean is provided both area-integrated and per area. The variable stoichiometry configurations also include the per area difference with respect to the RS configuration.

Annual subarea-integrated air-sea CO <sub>2</sub> exchange averaged over 2000–2010												
Subarea	RS		ER			PR			ER&PR			
	Total [TmolC yr <sup>-1</sup> ]	Per Area [molC m <sup>-2</sup> yr <sup>-1</sup> ]	Total [TmolC yr <sup>-1</sup> ]	Per Area [molC m <sup>-2</sup> yr <sup>-1</sup> ]	Difference [molC m <sup>-2</sup> yr <sup>-1</sup> ]	Total [TmolC yr <sup>-1</sup> ]	Per Area [molC m <sup>-2</sup> yr <sup>-1</sup> ]	Difference [molC m <sup>-2</sup> yr <sup>-1</sup> ]	Total [TmolC yr <sup>-1</sup> ]	Per Area [molC m <sup>-2</sup> yr <sup>-1</sup> ]	Difference [molC m <sup>-2</sup> yr <sup>-1</sup> ]	
Entire NWES	1.105	0.900	1.444	1.176	+0.276	1.207	0.984	+0.083	1.316	1.072	+0.171	
Entire North Sea	0.670	1.110	0.889	1.474	+0.364	0.736	1.221	+0.110	0.812	1.346	+0.236	
northern North Sea	0.156	1.977	0.187	2.379	+0.402	0.162	2.063	+0.085	0.174	2.211	+0.234	
central North Sea	0.331	1.361	0.445	1.833	+0.472	0.363	1.495	+0.134	0.407	1.673	+0.312	
southern North Sea	0.087	0.425	0.135	0.661	+0.236	0.106	0.522	+0.097	0.121	0.596	+0.171	
Norwegian Trench	0.097	1.245	0.122	1.570	+0.325	0.104	1.341	+0.095	0.110	1.414	+0.168	
English Channel	0.056	0.685	0.058	0.702	+0.017	0.057	0.691	+0.007	0.057	0.692	+0.008	
Skagerrak Kattegat	-0.051	-0.651	-0.042	-0.537	+0.114	-0.048	-0.615	+0.036	-0.046	-0.588	+0.063	
NE Celtic Sea	0.085	0.790	0.101	0.945	+0.155	0.088	0.817	+0.028	0.094	0.873	+0.083	
SW Celtic Sea	0.105	1.145	0.135	1.480	+0.335	0.116	1.272	+0.127	0.124	1.357	+0.212	
Irish Sea	0.001	0.028	-0.001	-0.017	-0.045	-0.001	-0.020	-0.048	-0.001	-0.030	-0.058	
Inner Seas (Scotland)	0.023	0.522	0.025	0.562	+0.040	0.023	0.530	+0.008	0.024	0.532	+0.010	
Armorican Shelf	0.044	0.624	0.073	1.039	+0.416	0.056	0.805	+0.181	0.062	0.892	+0.268	
Hebrides Shelf	0.069	1.939	0.079	2.227	+0.289	0.071	1.992	+0.054	0.074	2.095	+0.156	
Malin Shelf	0.037	1.757	0.044	2.063	+0.306	0.038	1.794	+0.037	0.040	1.903	+0.146	
West Irish Shelf	0.066	1.408	0.082	1.752	+0.343	0.071	1.503	+0.095	0.076	1.608	+0.200	

**Table S16:** Polynomial fit coefficients for seasonally and subarea-averaged vertical profiles of DIC, PO<sub>4</sub> and NO<sub>3</sub> in Fig. 12 and S15. Each variable is given by a function  $f(\mathbf{z})$  as defined below with depth  $\mathbf{z}$  and polynomial coefficients  $C_N$ .

Polynomial fit coefficients of function $f(z)$ for seasonally and subarea-averaged vertical profiles of DIC, PO <sub>4</sub> and NO <sub>3</sub>									
$f(z) = C_5 \times z^5 + C_4 \times z^4 + C_3 \times z^3 + C_2 \times z^2 + C_1 \times z^1 + C_0$									
Variable	Subarea	Season	$C_5$	$C_4$	$C_3$	$C_2$	$C_1$	$C_0$	
DIC	Mean	NT	Winter (DJF)	$-8.501 \times 10^{-11}$	$-1.081 \times 10^{-7}$	$-4.813 \times 10^{-5}$	$-8.865 \times 10^{-3}$	$-7.422 \times 10^{-1}$	2155.466
			Spring (MAM)	$-6.082 \times 10^{-10}$	$-6.708 \times 10^{-7}$	$-2.746 \times 10^{-4}$	$-5.125 \times 10^{-2}$	$-4.264$	2071.123
			Summer (JJA)	$-3.553 \times 10^{-10}$	$-4.544 \times 10^{-7}$	$-2.158 \times 10^{-4}$	$-4.683 \times 10^{-2}$	$-4.581$	2053.557
			Autumn (SON)	$-1.250 \times 10^{-10}$	$-1.764 \times 10^{-7}$	$-9.315 \times 10^{-5}$	$-2.294 \times 10^{-2}$	$-2.685$	2087.112
		NNS + CNS	Winter (DJF)	$1.307 \times 10^{-11}$	$1.787 \times 10^{-8}$	$8.678 \times 10^{-6}$	$1.732 \times 10^{-3}$	$1.283 \times 10^{-1}$	6.088
			Spring (MAM)	$1.062 \times 10^{-10}$	$1.390 \times 10^{-7}$	$6.476 \times 10^{-5}$	$1.324 \times 10^{-2}$	$1.165$	37.925
			Summer (JJA)	$-3.300 \times 10^{-11}$	$-3.122 \times 10^{-8}$	$-8.317 \times 10^{-6}$	$1.009 \times 10^{-4}$	$2.911 \times 10^{-1}$	29.286
			Autumn (SON)	$-1.119 \times 10^{-11}$	$-1.588 \times 10^{-8}$	$-8.153 \times 10^{-6}$	$-1.746 \times 10^{-3}$	$-1.029 \times 10^{-1}$	8.571
	SD	NT	Winter (DJF)	$1.731 \times 10^{-8}$	$5.925 \times 10^{-6}$	$7.261 \times 10^{-4}$	$3.926 \times 10^{-2}$	$8.554 \times 10^{-1}$	2174.176
			Spring (MAM)	$5.204 \times 10^{-8}$	$1.950 \times 10^{-5}$	$2.563 \times 10^{-3}$	$1.341 \times 10^{-1}$	$1.749$	2146.274
			Summer (JJA)	$4.971 \times 10^{-8}$	$2.015 \times 10^{-5}$	$2.854 \times 10^{-3}$	$1.580 \times 10^{-1}$	$1.676$	2119.107
			Autumn (SON)	$2.894 \times 10^{-8}$	$1.159 \times 10^{-5}$	$1.640 \times 10^{-3}$	$9.021 \times 10^{-2}$	$4.800 \times 10^{-1}$	2119.163
		NNS + CNS	Winter (DJF)	$-4.945 \times 10^{-9}$	$-1.923 \times 10^{-6}$	$-2.668 \times 10^{-4}$	$-1.574 \times 10^{-2}$	$-3.270 \times 10^{-1}$	3.823
			Spring (MAM)	$7.860 \times 10^{-10}$	$4.200 \times 10^{-7}$	$8.976 \times 10^{-5}$	$9.472 \times 10^{-3}$	$5.431 \times 10^{-1}$	17.771
			Summer (JJA)	$8.581 \times 10^{-9}$	$3.947 \times 10^{-6}$	$6.208 \times 10^{-3}$	$3.719 \times 10^{-2}$	$6.910 \times 10^{-1}$	16.854
			Autumn (SON)	$3.858 \times 10^{-8}$	$1.471 \times 10^{-5}$	$1.993 \times 10^{-3}$	$1.126 \times 10^{-1}$	$2.417$	27.440
PO <sub>4</sub>	Mean	NNS + CNS	Winter (DJF)	$1.543 \times 10^{-11}$	$5.092 \times 10^{-9}$	$4.692 \times 10^{-7}$	$1.669 \times 10^{-5}$	$8.289 \times 10^{-4}$	$6.420 \times 10^{-1}$
			Spring (MAM)	$1.295 \times 10^{-11}$	$4.443 \times 10^{-9}$	$2.278 \times 10^{-7}$	$-3.684 \times 10^{-5}$	$-3.438 \times 10^{-3}$	$3.455 \times 10^{-1}$
			Summer (JJA)	$2.356 \times 10^{-10}$	$1.011 \times 10^{-7}$	$1.531 \times 10^{-5}$	$9.266 \times 10^{-4}$	$1.236 \times 10^{-2}$	$1.828 \times 10^{-1}$
			Autumn (SON)	$-3.862 \times 10^{-11}$	$-1.422 \times 10^{-8}$	$-9.474 \times 10^{-7}$	$1.247 \times 10^{-4}$	$9.711 \times 10^{-3}$	$5.298 \times 10^{-1}$
	SD	NNS + CNS	Winter (DJF)	$4.952 \times 10^{-11}$	$2.624 \times 10^{-8}$	$5.055 \times 10^{-6}$	$4.170 \times 10^{-4}$	$1.303 \times 10^{-2}$	$1.930 \times 10^{-1}$
			Spring (MAM)	$2.932 \times 10^{-12}$	$6.676 \times 10^{-10}$	$3.308 \times 10^{-8}$	$1.007 \times 10^{-5}$	$2.239 \times 10^{-3}$	$1.656 \times 10^{-1}$
			Summer (JJA)	$3.750 \times 10^{-11}$	$1.584 \times 10^{-8}$	$2.202 \times 10^{-6}$	$9.837 \times 10^{-5}$	$2.461 \times 10^{-4}$	$1.187 \times 10^{-1}$
			Autumn (SON)	$-2.413 \times 10^{-11}$	$-1.177 \times 10^{-8}$	$-1.909 \times 10^{-6}$	$-1.087 \times 10^{-4}$	$-9.343 \times 10^{-4}$	$1.350 \times 10^{-1}$
NO <sub>3</sub>	Mean	NNS + CNS	Winter (DJF)	$-3.479 \times 10^{-10}$	$-1.539 \times 10^{-7}$	$-2.202 \times 10^{-5}$	$-8.834 \times 10^{-4}$	$1.298 \times 10^{-2}$	8.414
			Spring (MAM)	$1.271 \times 10^{-9}$	$6.194 \times 10^{-7}$	$1.096 \times 10^{-4}$	$8.300 \times 10^{-3}$	$1.842 \times 10^{-1}$	4.268
			Summer (JJA)	$-6.435 \times 10^{-10}$	$-3.310 \times 10^{-7}$	$-5.331 \times 10^{-5}$	$-3.027 \times 10^{-3}$	$-1.045 \times 10^{-1}$	$5.854 \times 10^{-1}$
			Autumn (SON)	$-5.051 \times 10^{-10}$	$-2.309 \times 10^{-7}$	$-2.912 \times 10^{-5}$	$-3.413 \times 10^{-4}$	$4.106 \times 10^{-2}$	5.507
	SD	NNS + CNS	Winter (DJF)	$4.146 \times 10^{-10}$	$2.243 \times 10^{-7}$	$4.467 \times 10^{-5}$	$3.863 \times 10^{-3}$	$1.315 \times 10^{-1}$	2.406
			Spring (MAM)	$9.102 \times 10^{-10}$	$4.563 \times 10^{-7}$	$8.320 \times 10^{-5}$	$6.706 \times 10^{-3}$	$2.320 \times 10^{-1}$	3.504
			Summer (JJA)	$1.081 \times 10^{-9}$	$4.807 \times 10^{-7}$	$7.366 \times 10^{-5}$	$4.320 \times 10^{-3}$	$7.011 \times 10^{-2}$	1.109
			Autumn (SON)	$6.768 \times 10^{-11}$	$9.436 \times 10^{-8}$	$3.034 \times 10^{-5}$	$3.737 \times 10^{-3}$	$1.827 \times 10^{-1}$	3.542

## S2 Ecosystem model equations: variable stoichiometry ECOSMO II

The here introduced variable stoichiometry version of ECOSMO II is an extension to the model presented in Daewel and Schrum (2013). Dissolved and particulate organic matter, formerly constrained to constant Redfield stoichiometry (Redfield, 1963), are now separated into individual variables for carbon, nitrogen, and phosphorus contents in both pelagic and benthic reservoirs. While primary and secondary production remain at Redfield stoichiometry, we here introduce two pathways for variable organic matter stoichiometry: firstly, we allow for carbon fixation beyond nutrient limitation in form of an extracellular release of carbon-enriched dissolved organic matter. This implementation represents the release of carbohydrates observed in phytoplankton blooms under nutrient stress (Børshem et al., 2005; Fajon et al., 1999; Søndergaard et al., 2000) and was adapted from the model parametrization in Neumann et al. (2022). With this, we also include the suggested particle formation from dissolved to particulate organic matter as transparent exopolymer particles (Engel, 2002; Neumann et al., 2022), and add a dependence on the nutrient state as for the DIC uptake by the extracellular release itself. Secondly, we consider the observed preferential remineralization of nitrogen and phosphorus with the sequence P > N > C (Clark et al., 1998; Hopkinson et al., 2002; Loh and Bauer, 2000; Thomas et al., 1999; Williams et al., 1980) with a constant ratio between the remineralization rates of carbon, nitrogen and phosphorus. By considering variable stoichiometry in the production and degradation of organic matter, the model can represent variations in organic matter composition and their control on the coupling of elemental fluxes. It further incorporates the additional variables dissolved inorganic carbon (DIC) and total alkalinity (TA) introduced in Kossack et al. (2024) for the coupling to a carbonate system model (Blackford and Gilbert, 2007). This enables the analysis of the effects of variable stoichiometry on inorganic carbon contents and carbon cycling.

The model integrates a total of twenty-four prognostic equations for tracer concentrations of different functional groups. Besides DIC and TA, these include three phytoplankton (flagellates, diatoms, and cyanobacteria), two zooplankton (micro- and meso-zooplankton), seven detritus (pelagic DOC, DON, DOP, POC, PON, POP, and biogenic opal), five sediment (benthic POC, PON, POP, PIP, and opal), and four nutrient variables ( $\text{NO}_3^-$ ,  $\text{NH}_4^+$ ,  $\text{PO}_4^{3-}$ ,  $\text{SiO}_2$ ) in addition to oxygen. Each tracer concentration  $C$  is integrated in time based on a prognostic equation of the form:

$$(1) \quad C_t + (\nu \cdot \nabla)C + w_d C_z = (A_\nu C_z)_z + R_C,$$

where subscripts of time  $t$  and depth  $z$  represent derivatives  $d/dt$  and  $d/dz$  respectively. Here,  $\nu=(u, v, w)$  is the three-dimensional velocity field,  $A_\nu$  the sub-scale diffusion coefficient,  $w_d$  a constant sinking velocity and  $R_C$  the local sources and sinks. The sinking velocity  $w_d$  is only non-zero for particulate organic matter, cyanobacteria, and opal. Whereas the physical model component provides physical transports by advection  $(\nu \cdot \nabla)C$ , diffusion  $(A_\nu C_z)_z$ , and sinking  $w_d C_z$ , the ECOSMO II module describes the biogeochemical processes in  $R_C$  that act as local sources and sinks. The table below summarizes these terms  $R_C$  for all twenty-four tracers. For a more detailed description of the primary production, secondary

production, and nutrient limitation dynamics, the reader is referred to the original ECOSMO II model description (Daewel and Schrum, 2013).

Local sink and source terms $R_C$ for all tracer concentrations $C_X$ of tracer $X$		
Variable	Definition	Unit
Primary Production		
$C_{P_1}$ : biomass of phytoplankton group $P_j$	$R_{P_j} = \sigma_j \beta_{T_j} \Phi_{P_j} C_{P_j} - \sum_{i=1}^2 G_i(C_{P_j}) C_{Z_i} - m_{P_j} C_{P_j}$ for $j$ in [1, 2, 3]	[mg C m <sup>-3</sup> ]
$C_{P_1}$ : flagellate biomass	$\Phi_{P_1} = \min(\alpha(I), \beta_N, \beta_P)$	[mg C m <sup>-3</sup> ]
$C_{P_2}$ : diatom biomass	$\Phi_{P_2} = \min(\alpha(I), \beta_N, \beta_P, \beta_{Si})$	[mg C m <sup>-3</sup> ]
$C_{P_3}$ : cyanobacteria biomass	$\Phi_{P_3} = \begin{cases} 0, & \text{if } C_{Sal} > 10.0 \text{ or } I_s(x, y) < 120 \text{ W m}^{-2} \\ \min(\alpha(I), \beta_P), & \text{else if } n_z = N_z \\ \min(\alpha(I), \beta_N, \beta_P), & \text{else} \end{cases}$ with $C_{Sal}$ provided by the physical model.	[mg C m <sup>-3</sup> ]
$\alpha(I)$ : light limitation	$\alpha(I) = \tanh(a \cdot I(x, y, z, t))$	-
$I(x, y, z, t)$ : photosynthetically active radiation	$I(x, y, z, t) = \frac{I_0(x, y)}{2} \exp(-k_w z - k_{phyto} \int_z^0 \sum_{j=1}^3 C_{P_j} \partial z)$	[W m <sup>-2</sup> ]
$\beta_N$ : nitrogen limitation	$\beta_N = \beta_{NH_4} + \beta_{NO_3}$	-
$\beta_{NH_4}$ : ammonium limitation	$\beta_{NH_4} = \frac{C_{NH_4}}{r_{NH_4} + C_{NH_4}}$	-
$\beta_{NO_3}$ : nitrate limitation	$\beta_{NO_3} = \frac{C_{NO_3}}{r_{NO_3} + C_{NO_3}} \exp(-\Psi \cdot C_{NH_4})$	-
$\beta_P$ : phosphorus limitation	$\beta_P = \frac{C_{PO_4}}{r_{PO_4} + C_{PO_4}}$	-
$\beta_{Si}$ : silicate limitation	$\beta_{Si} = \max(0, \frac{C_{SiO_2} - R_{SiO_2}}{r_{SiO_2} + C_{SiO_2}})$	-
$\beta_{T_{1,2,3}}$ : temperature dependence	$\beta_{T_1} = 1, \beta_{T_2} = 1, \beta_{T_3}(T) = \frac{1}{1 + \exp(-T)}$	-
$\sigma_{P_j}$ : maximum growth rate of phytoplankton group $P_j$	$\sigma_{P_1} = 1.10, \sigma_{P_2} = 1.30, \sigma_{P_3} = 1.00$	[d <sup>-1</sup> ]
$m_{P_j}$ : mortality rate of phytoplankton group $P_j$	$m_{P_1} = 0.08, m_{P_2} = 0.05, m_{P_3} = 0.08$	[d <sup>-1</sup> ]
$I_s(x, y)$ : short wave radiation	Prescribed fields loaded from file.	[W m <sup>-2</sup> ]
$\alpha$ : Photosynthesis efficiency	$\alpha = 0.01$	[(W m <sup>-2</sup> ) <sup>-1</sup> ]
$k_w$ : water background light extinction coefficient	$k_w = 0.05$	[m <sup>-1</sup> ]
$k_{phyto}$ : phytoplankton light extinction coefficient	$k_{phyto} = 0.20$	[m <sup>2</sup> (mmol C) <sup>-1</sup> ]
$\Psi$ : NH <sub>4</sub> inhibition parameter	$\Psi = 3.00$	[m <sup>3</sup> (mmol N) <sup>-1</sup> ]

$r_{NO_3}$ : $NO_3$ half saturation constant	$r_{NO_3} = 0.50$	$[mmol\ N\ m^{-3}]$
$r_{NH_4}$ : $NH_4$ half saturation constant	$r_{NH_4} = 0.20$	$[mmol\ N\ m^{-3}]$
$r_{PO_4}$ : $PO_4$ half saturation constant	$r_{PO_4} = 0.05$	$[mmol\ P\ m^{-3}]$
$r_{SiO_2}$ : $SiO_2$ half saturation constant	$r_{SiO_2} = 0.50$	$[mmol\ Si\ m^{-3}]$
Rr <sub>SiO<sub>2</sub></sub> : $SiO_2$ constant	Rr <sub>SiO<sub>2</sub></sub> = 1.00	$[mmol\ Si\ m^{-3}]$
Secondary Production		
$C_{Z_1}$ : micro-zooplankton biomass	$R_{Z_1} = \gamma_1 C_{Z_1} \sum_{j=1}^3 G_1(C_{P_j}) + \gamma_2 G_1(\min(C_{POC}, C_{PON}, C_{POP})) C_{Z_1} - G_2(C_{Z_1}) C_{Z_2} - \mu_1 C_{Z_1} - m_{Z_1} C_{Z_1}$	$[mg\ C\ m^{-3}]$
$C_{Z_2}$ : meso-zooplankton biomass	$R_{Z_2} = \gamma_1 C_{Z_2} \sum_{j=1}^3 G_2(C_{P_j}) + \gamma_2 G_2(\min(C_{POC}, C_{PON}, C_{POP})) C_{Z_2} - \mu_2 C_{Z_2} - m_{Z_2} C_{Z_2}$	$[mg\ C\ m^{-3}]$
$G_i(C_X)$ : zooplankton grazing rates	$G_i(C_X) = \sigma_{i,X} \frac{a_{iX} C_X}{r_i + H_i}$ with $H_i = \sum_X a_{iX} C_X$	-
$r_Z$ : zooplankton half saturation constant	$r_Z = 3.3$	$[mmol\ C\ m^{-3}]$
$m_{Z_i}$ : zooplankton mortality rate of group $Z_i$	$m_{Z_1} = 0.2, m_{Z_2} = 0.1$	$[d^{-1}]$
$\mu_{Z_i}$ : zooplankton excretion rate of group $Z_i$	$\mu_{Z_1} = 0.08, \mu_{Z_2} = 0.06$	$[d^{-1}]$
$\gamma_1$ : assimilation efficiency of grazing on $P_{1,2,3}$ and $Z_1$	$\gamma_1 = 0.75$	-
$\gamma_2$ : assimilation efficiency of grazing on POC	$\gamma_2 = 0.30$	-
$\sigma_{Z_1,X}$ : grazing parameter of $Z_1$ on $X$	$\sigma_{Z_1,P_1} = 1.00, \sigma_{Z_1,P_2} = 1.00, \sigma_{Z_1,P_3} = 0.30, \sigma_{Z_1,Z_1} = 0.00, \sigma_{Z_1,POC} = 1.00$	-
$a_{Z_1,X}$ : grazing parameter of $Z_1$ on $X$	$a_{Z_1,P_1} = 0.70, a_{Z_1,P_2} = 0.25, a_{Z_1,P_3} = 0.30, a_{Z_1,Z_1} = 0.00, a_{Z_1,POC} = 0.10$	-
$\sigma_{Z_2,X}$ : grazing parameter of $Z_2$ on $X$	$\sigma_{Z_2,P_1} = 0.80, \sigma_{Z_2,P_2} = 0.80, \sigma_{Z_2,P_3} = 0.30, \sigma_{Z_2,Z_1} = 0.50, \sigma_{Z_2,POC} = 0.80$	-
$a_{Z_2,X}$ : grazing parameter of $Z_2$ on $X$	$a_{Z_2,P_1} = 0.10, a_{Z_2,P_2} = 0.85, a_{Z_2,P_3} = 0.30, a_{Z_2,Z_1} = 0.15, a_{Z_2,POC} = 0.10$	-
Degradation Products		
$C_{DOC}$ : dissolved organic carbon concentration	$R_{DOC} = a_{DOM} R_{OM}^+ - \epsilon_{DOC} C_{DOC} + E_{DOC} - F_{DOC2POC}$	$[mg\ C\ m^{-3}]$
$C_{DON}$ : dissolved organic nitrogen concentration	$R_{DON} = a_{DOM} R_{OM}^+ - \epsilon_{DON} C_{DON} + E_{DON} - F_{DON2PON}$	$[mg\ C\ m^{-3}]$
$C_{DOP}$ : dissolved organic phosphorus concentration	$R_{DOP} = a_{DOM} R_{OM}^+ - \epsilon_{DOP} C_{DOP} + E_{DOP} - F_{DOP2POP}$	$[mg\ C\ m^{-3}]$
$C_{POC}$ : particulate organic carbon concentration	$R_{POC} = (1 - a_{DOM}) R_{OM}^+ - R_{POC}^- + \left[ \frac{\lambda_{res} C_{Sed,POC} - \lambda_{dep} C_{POC}}{dz} \right]_{n_z=0} + F_{DOC2POC}$	$[mg\ C\ m^{-3}]$
$C_{PON}$ : particulate organic nitrogen concentration	$R_{PON} = (1 - a_{DOM}) R_{OM}^+ - R_{PON}^- + \left[ \frac{\lambda_{res} C_{Sed,PON} - \lambda_{dep} C_{PON}}{dz} \right]_{n_z=0} + F_{DON2PON}$	$[mg\ C\ m^{-3}]$

$C_{\text{POP}}$ : particulate organic phosphorus concentration	$R_{\text{POP}} = (1 - \alpha_{\text{DOM}})R_{\text{OM}}^+ - R_{\text{POP}}^- + \left[ \frac{\lambda_{\text{res}} C_{\text{Sed,POP}} - \lambda_{\text{dep}} C_{\text{POP}}}{dz} \right]_{n_z=0} + F_{\text{DOP2POP}}$	[mg C m <sup>-3</sup> ]
$C_{\text{opal}}$ : biogenic opal concentration	$R_{\text{Opal}} = \frac{1}{\text{REF}_{\text{C,SI}}} \left[ \sum_{i=1}^2 G_i(P_2) C_{Z_i} + m_2 P_2 - \epsilon_{\text{Si}} C_{\text{Opal}} \right] + \left[ \frac{\lambda_{\text{res}} C_{\text{Sed,SIo}_2} - \lambda_{\text{dep}} C_{\text{Opal}}}{dz} \right]_{n_z=0}$	[mg C m <sup>-3</sup> ]
$R_{\text{OM}}^+$ : new detrital matter from assimilation losses and mortality	$R_{\text{OM}}^+ = (1 - \gamma_1) \left( \sum_{i=1}^2 C_{Z_i} \sum_{j=1}^3 G_i(C_{P_j}) + G_2(C_{Z_1}) \right) + (1 - \gamma_2) \sum_{i=1}^2 C_{Z_i} G_i(\min(C_{\text{POC}}, C_{\text{PON}}, C_{\text{POP}})) + \sum_{j=1}^3 m_{P_j} C_{P_j} + \sum_{i=1}^2 m_{Z_i} C_{Z_i}$	[mg C m <sup>-3</sup> s <sup>-1</sup> ]
$R_X^-$ : POM losses through grazing and remineralization	$R_X^- = \sum_{i=1}^2 C_{Z_i} G_i(\min(C_{\text{POC}}, C_{\text{PON}}, C_{\text{POP}})) + \epsilon_X(T) C_X$ for $X$ in [POC, PON, POP]	[mg C m <sup>-3</sup> s <sup>-1</sup> ]
$\epsilon_{\text{POC}}(T)$ : remineralization rate of POC	$\epsilon_{\text{POC}}(T) = 0.006 \times (1 + 20 \times (\frac{T^2}{T_{\text{ref}}^2 + T^2}))$	[d <sup>-1</sup> ]
$\epsilon_{\text{PON}}(T)$ : remineralization rate of PON	$\epsilon_{\text{PON}}(T) = \frac{\epsilon_{\text{POC}}(T)}{\epsilon_{\text{POC:PON}}}$ with parameter $\epsilon_{\text{POC:PON}}$ specified in configuration	[d <sup>-1</sup> ]
$\epsilon_{\text{POP}}(T)$ : remineralization rate of POP	$\epsilon_{\text{POP}}(T) = \frac{\epsilon_{\text{POC}}(T)}{\epsilon_{\text{POC:POP}}}$ with parameter $\epsilon_{\text{POC:POP}}$ specified in configuration	[d <sup>-1</sup> ]
$\epsilon_{\text{DOC}}(T)$ : remineralization rate of DOC	$\epsilon_{\text{DOC}}(T) = \epsilon_{\text{DOC:POC}} \epsilon_{\text{POC}}(T)$ with parameter $\epsilon_{\text{DOC:POC}}$ specified in configuration	[d <sup>-1</sup> ]
$\epsilon_{\text{DON}}(T)$ : remineralization rate of DON	$\epsilon_{\text{DON}}(T) = \frac{\epsilon_{\text{DOC}}(T)}{\epsilon_{\text{DOC:DON}}}$ with parameter $\epsilon_{\text{DOC:DON}}$ specified in configuration	[d <sup>-1</sup> ]
$\epsilon_{\text{DOP}}(T)$ : remineralization rate of DOP	$\epsilon_{\text{DOP}}(T) = \frac{\epsilon_{\text{DOC}}(T)}{\epsilon_{\text{DOC:DOP}}}$ with parameter $\epsilon_{\text{DOC:DOP}}$ specified in configuration	[d <sup>-1</sup> ]
$\epsilon_{\text{Si}}$ : remineralization rate of opal	$\epsilon_{\text{Si}} = 0.015$	[d <sup>-1</sup> ]
$\alpha_{\text{DOM}}$ : fraction of dissolved organic matter from new detrital matter	$\alpha_{\text{DOM}} = 0.4$	-
$T_{\text{ref}}$ : reference temperature for remineralization	$T_{\text{ref}} = 13$	[°C]
$w_D$ : sinking rate of particulate organics and opal	$w_D = 5$	[md <sup>-1</sup> ]
$n_z$ : depth index with bottom index $n_z = 0$ , surface index $n_z = N_z$	Provided by the physical model component.	-
$dz$ : vertical step size at depth level $n_z$	Provided by the physical model component.	[m]

#### Extracellular Release and Flocculation

$E$ : extracellular release base rate	$E = B_{\text{ER}} \times \sum_{j=1}^3 (\sigma_j C_{P_j} \beta_{Tj})$ with temperature limitation $\beta_{Tj}$ of phytoplankton group $P_j$ where applicable	[mg C m <sup>-3</sup> s <sup>-1</sup> ]
$E_{\text{DON}}$ : extracellular release of DON	$E_{\text{DON}} = \begin{cases} E \times \min(1 - \beta_P, \beta_N, \alpha(I)), & \beta_P > 0.1 \text{ and } \beta_P < 1 \\ 0, & \beta_N \leq 0.1 \text{ or } \beta_P \geq 1 \end{cases}$	[mg C m <sup>-3</sup> s <sup>-1</sup> ]
$E_{\text{DOP}}$ : extracellular release of DOP	$E_{\text{DOP}} = \begin{cases} E \times \min(\beta_P, 1.1 - \beta_N, \alpha(I)), & \beta_P > 0.1 \text{ and } \beta_N < 1.1 \\ 0, & \beta_P \leq 0.1 \text{ or } \beta_N \geq 1.1 \end{cases}$	[mg C m <sup>-3</sup> s <sup>-1</sup> ]
$E_{\text{DOC}}$ : extracellular release of DOC	$E_{\text{DOC}} = E_{\text{DON}} + E_{\text{DOP}} + \begin{cases} E \times \min(\max(1 - \beta_P, 1.1 - \beta_N), \alpha(I)), & \beta_P < 1 \text{ and } \beta_N < 1.1 \\ 0, & \beta_P \geq 1 \text{ or } \beta_N \geq 1.1 \end{cases}$	[mg C m <sup>-3</sup> s <sup>-1</sup> ]
$F$ : flocculation base rate	$F = F_{\text{DOM2POM}} \times B_{\text{ER}}$	[s <sup>-1</sup> ]
$F_{\text{DON2PON}}$ : flocculation from DON to PON	$F_{\text{DON2PON}} = \begin{cases} F \times C_{\text{DON}} \times \min(1 - \beta_P, \beta_N, \alpha(I)), & \beta_N > 0.1 \text{ and } \beta_P < 1 \\ 0, & \beta_N \leq 0.1 \text{ or } \beta_P \geq 1 \end{cases}$	[mg C m <sup>-3</sup> s <sup>-1</sup> ]

$F_{DOP2POP}$ : flocculation from DOP to POP	$F_{DOP2POP} = \begin{cases} F \times C_{DOP} \times \min(\beta_P, 1.1 - \beta_N, \alpha(I)), & \beta_P > 0.1 \text{ and } \beta_N < 1.1 \\ 0, & \beta_P \leq 0.1 \text{ or } \beta_N \geq 1.1 \end{cases}$	[mg C m <sup>-3</sup> s <sup>-1</sup> ]
$F_{DOC2POC}$ : flocculation from DOC to POC	$F_{DOC2POC} = F_{DON2PON} + F_{DOP2POP} + \begin{cases} F \times C_{DOC} \times \min(\max(1 - \beta_P, 1.1 - \beta_N), \alpha(I)), & \beta_P < 1 \text{ and } \beta_N < 1.1 \\ 0, & \beta_P \geq 1 \text{ or } \beta_N \geq 1.1 \end{cases}$	[mg C m <sup>-3</sup> s <sup>-1</sup> ]
$B_{ER}$ : extracellular release scaling factor	Specified in configuration.	-
$F_{DOM2POM}$ : flocculation scaling factor	Specified in configuration.	[d <sup>-1</sup> ]
Nutrients		
$C_{NH_4}$ : ammonium concentration	$R_{NH_4} = -\frac{\beta_{NH_4}}{\beta_N} (\sum_{j=1}^3 \sigma_j \beta_{Tj} \Phi_{Pj} C_{Pj} + E_{DON}) + \sum_{i=1}^2 \mu_i C_{Zi} + \epsilon_{PON} C_{PON} + \epsilon_{DON} C_{DON} - \Omega_a(O_2, T) C_{NH_4} + \left[ \frac{C_{Sed.PON} \theta(O_2) \epsilon_{Sed.Ox}}{dz} \right]_{n_z=0} + \left[ \frac{\theta(-O_2) \epsilon_{Sed.Anox}}{dz} \right]_{n_z=0} + SurfNH_4$ with surface deposition SurfNH <sub>4</sub> provided from observational data.	[mg C m <sup>-3</sup> ]
$C_{NO_3}$ : nitrate concentration	$R_{NO_3} = -\frac{\beta_{NO_3}}{\beta_N} (\sum_{j=1}^3 \sigma_j \beta_{Tj} \Phi_{Pj} C_{Pj} + E_{DON}) + \Omega_a(O_2, T) C_{NH_4} - \theta(-O_2) \theta(NO_3) a_{denit} (\epsilon_{POC} C_{POC} + \epsilon_{DOC} C_{DOC}) - \left[ \frac{-\theta(-O_2) \theta(NO_3) a_{denit} \epsilon_{Sed.Anox} C_{Sed.PON}}{dz} \right]_{n_z=0} + SurfNO_3$ with surface deposition SurfNO <sub>3</sub> provided from observational data.	[mg C m <sup>-3</sup> ]
$C_{PO_4}$ : phosphate concentration	$R_{PO_4} = -\sum_{j=1}^3 \sigma_j \beta_{Tj} \Phi_{Pj} C_{Pj} - E_{DOP} + \epsilon_{POP} C_{POP} + \epsilon_{DOP} C_{DOP} + \sum_{i=1}^2 \mu_i C_{Zi} + \left[ \frac{\theta(O_2) \epsilon_p (1 - 0.15\sigma) C_{Sed.PIP}}{dz} \right]_{n_z=0} + \left[ \frac{\theta(-O_2) \epsilon_{PIP} C_{Sed.PIP}}{dz} \right]_{n_z=0}$	[mg C m <sup>-3</sup> ]
$C_{SiO_2}$ : silicate concentration	$R_{SiO_2} = -\Phi_2 \sigma_2 P_2 + \epsilon_{Si} C_{Opal} + \left[ \frac{\epsilon_{Sed.SiO_2} C_{Sed.SiO_2}}{dz} \right]_{n_z=0}$	[mg C m <sup>-3</sup> ]
$C_{O_2}$ : oxygen concentration	$R_{O_2} = \frac{1}{REDF_{C,O_2} REDF_{C,N}} \left( \frac{6.625\beta_{NH_4} + 8.125\beta_{NO_3}}{\beta_N} \sum_{j=1}^3 \sigma_j \beta_{Tj} \Phi_{Pj} C_{Pj} - \theta(O_2) (6.625(\epsilon_{POC} C_{POC} + \epsilon_{DOC} C_{DOC}) + \sum_{i=1}^2 \mu_i C_{Zi}) + 2\Omega_a(O_2, T) C_{NH_4} \right) + \frac{E_{DOC}}{REDF_{C,O_2}} + SurfO_2 + BottomO_2$	[mmol O <sub>2</sub> m <sup>-3</sup> ]
$\Omega_a(O_2, T)$ : oxygen and temperature scaling	$\Omega_a(O_2, T) = 0.1 \times \theta(O_2) \exp(0.11 \times T) \frac{C_{O_2}}{0.01 + C_{O_2}}$	-
$\theta(x)$ : distinction for oxygen and nitrogen conditions	$\theta(x) = \begin{cases} 1, & \forall x > 0 \\ 0, & \forall x \leq 0 \end{cases}$	-
SurfO <sub>2</sub> : air-sea O <sub>2</sub> exchange	$SurfO_2 = \left[ \frac{\nu_P}{dz(O_{2sat}(T,S) - C_{O_2})} \right]_{n_z=N_z}$	[mmol O <sub>2</sub> m <sup>-3</sup> d <sup>-1</sup> ]
BottomO <sub>2</sub> : benthic-pelagic O <sub>2</sub> exchange flux	$BottomO_2 = - \left[ \frac{\theta(O_2)(2 \times 6.625 \times \epsilon_{Sed.Ox} C_{Sed.POC} + \Omega_a(O_2, T) \epsilon_{Sed.Ox} C_{Sed.POC})}{dz REDF_{C,O_2} REDF_{C,N}} \right]_{n_z=0} - \left[ \frac{\theta(-O_2) \theta(-NO_3) 6.625 \times \epsilon_{Sed.Anox} C_{Sed.POC}}{dz REDF_{C,O_2} REDF_{C,N}} \right]_{n_z=0}$	[mmol O <sub>2</sub> m <sup>-3</sup> d <sup>-1</sup> ]
O <sub>2sat</sub> (T, S): oxygen saturation	$O_{2sat}(T, S) = \exp \left( -135.90205 + 1.575701 \times 10^5 \times T_{O_2} - 6.642308 \times 10^7 \times T_{O_2}^2 + 1.2438 \times 10^{10} \times T_{O_2}^3 - 8.621949 \times 10^{11} \times T_{O_2}^4 - C_{Sal} (1.7674 \times 10^{-2} - 10.754 \times T_{O_2} + 2140.7 \times T_{O_2}^2) \right)$ with $T_{O_2}(T) = \frac{1}{T+273.15}$	[mmol O <sub>2</sub> m <sup>-3</sup> ]
$a_{denit}$ : increased nitrate loss as oxidation agent under anoxic conditions	$a_{denit} = 5$	-
$\Omega_{aMax}$ : NH <sub>4</sub> maximum oxidation rate	$\Omega_{aMax} = 0.05$	[d <sup>-1</sup> ]
$\Omega_{nMax}$ : NO <sub>2</sub> maximum oxidation rate	$\Omega_{nMax} = 0.10$	[d <sup>-1</sup> ]
$\Omega_{rMax}$ : NO <sub>3</sub> maximum reduction rate	$\Omega_{rMax} = 0.01$	[d <sup>-1</sup> ]
$\Omega_{dMax}$ : NO <sub>2</sub> maximum reduction rate	$\Omega_{dMax} = 0.01$	[d <sup>-1</sup> ]

$v_p$ : oxygen piston velocity	$v_p = 5$	$[md^{-1}]$
$\text{REDF}_{\text{C:N}}$ : Redfield ratio of carbon to nitrogen	$\text{REDF}_{\text{C:N}} = 6.625$	$[\frac{\text{mol C}}{\text{mol N}}]$
$\text{REDF}_{\text{C:P}}$ : Redfield ratio of carbon to phosphorus	$\text{REDF}_{\text{C:P}} = 106$	$[\frac{\text{mol C}}{\text{mol P}}]$
$\text{REDF}_{\text{C:Si}}$ : Redfield ratio of carbon to silicon	$\text{REDF}_{\text{C:Si}} = 6.625$	$[\frac{\text{mol C}}{\text{mol Si}}]$
$\text{REDF}_{\text{C:O}_2}$ : molar mass of carbon	$\text{REDF}_{\text{C:O}_2} = 12.01$	$[\frac{g \text{ C}}{\text{mol C}}]$
Sediment Processes		
$C_{\text{Sed.POc}}$ : benthic POC concentration	$R_{\text{Sed.POc}} = \lambda_{\text{dep}} C_{\text{POC}} - C_{\text{Sed.POc}} (\lambda_{\text{res}} + \theta(O_2) 2\epsilon_{\text{Sed.Ox}} + \theta(-O_2) \epsilon_{\text{Sed.Anox}} + \delta_{\text{bur}})$	$[mg \text{ C m}^{-2}]$
$C_{\text{Sed.PON}}$ : benthic PON concentration	$R_{\text{Sed.PON}} = \lambda_{\text{dep}} C_{\text{PON}} - C_{\text{Sed.PON}} (\lambda_{\text{res}} + \theta(O_2) \epsilon_{\text{Sed.Ox}} + \theta(-O_2) \epsilon_{\text{Sed.Anox}} + \delta_{\text{bur}})$	$[mg \text{ C m}^{-2}]$
$C_{\text{Sed.POP}}$ : benthic POP concentration	$R_{\text{Sed.POP}} = \lambda_{\text{dep}} C_{\text{POP}} - C_{\text{Sed.POP}} (\lambda_{\text{res}} + \theta(O_2) 2\epsilon_{\text{Sed.Ox}} + \theta(-O_2) \epsilon_{\text{Sed.Anox}} + \delta_{\text{bur}})$	$[mg \text{ C m}^{-2}]$
$C_{\text{Sed.PIP}}$ : benthic inorganic iron-bound phosphate concentration	$R_{\text{Sed.PIP}} = \theta(O_2) (2\epsilon_{\text{Sed.Ox}} C_{\text{Sed.POP}} - \epsilon_{\text{PIP}} (1 - 0.15\sigma) C_{\text{Sed.PIP}}) + \theta(-O_2) (\epsilon_{\text{Sed.Anox}} C_{\text{Sed.POP}} - \epsilon_{\text{PIP}} C_{\text{Sed.PIP}})$	$[mg \text{ C m}^{-2}]$
$C_{\text{Sed.SiO}_2}$ : benthic opal concentration	$R_{\text{Sed.SiO}_2} = \lambda_{\text{dep}} C_{\text{Opal}} - C_{\text{Sed.SiO}_2} (\lambda_{\text{res}} + \epsilon_{\text{Sed.SiO}_2} + \delta_{\text{bur}})$	$[mg \text{ C m}^{-2}]$
$\epsilon_{\text{Sed.Ox}}(T)$ : organic sediment remineralization under oxic conditions	$\epsilon_{\text{Sed.Ox}}(T) = 0.001 \times \exp(0.15 \times T)$	$[d^{-1}]$
$\epsilon_{\text{Sed.Anox}}(T)$ : organic sediment remineralization under anoxic conditions	$\epsilon_{\text{Sed.Anox}}(T) = 2 \times \epsilon_{\text{Sed.Ox}}(T)$	$[d^{-1}]$
$\epsilon_{\text{PIP}}(T)$ : release of phosphate from benthic PIP into the water column	$\epsilon_{\text{PIP}}(T) = 2 \times \epsilon_{\text{Sed.Ox}}(T)$	$[d^{-1}]$
$\sigma$ : oxygen dependence of organic sediment phosphorous remineralization	$\sigma = \frac{\left(\frac{C_{O_2}}{375}\right)^2}{0.12 + \left(\frac{C_{O_2}}{375}\right)^2}$	-
$\epsilon_{\text{Sed.SiO}_2}$ : sediment opal remineralization rate	$\epsilon_{\text{Sed.SiO}_2} = 0.0002$	$[d^{-1}]$
$\lambda_{\text{dep}}$ : sedimentation rate below critical bottom shear stress	$\lambda_{\text{dep}} = \begin{cases} 3.5, & \tau < \tau_{\text{crit}} \\ 0, & \tau \geq \tau_{\text{crit}} \end{cases}$	$[d^{-1}]$
$\lambda_{\text{res}}$ : resuspension rate above critical bottom shear stress	$\lambda_{\text{res}} = \begin{cases} 0, & \tau < \tau_{\text{crit}} \\ 25, & \tau \geq \tau_{\text{crit}} \end{cases}$	$[d^{-1}]$
$\tau_{\text{crit}}$ : critical bottom shear stress	$\tau_{\text{crit}} = 0.007$	$[Nm^{-2}]$
$\delta_{\text{bur}}$ : burial rate	$\delta_{\text{pur}} = 10^{-5}$	$[d^{-1}]$
Carbonate System Variables		
$C_{\text{DIC}}$ : dissolved inorganic carbon concentration	$R_{\text{DIC}} = \frac{1}{\text{REDF}_{\text{C:O}_2}} (\sum_{i=1}^2 \mu_i C_{Z_i} + \epsilon_{\text{DOC}} C_{\text{DOC}} + \epsilon_{\text{POC}} C_{\text{POC}} - \sum_{j=1}^3 \sigma_j \beta_{T_j} \Phi_{P_j} C_{P_j} - E_{\text{DOC}}) + \frac{1}{\text{REDF}_{\text{C:O}_2}} \left[ \frac{\theta(O_2) (2\epsilon_{\text{Sed.Ox}} C_{\text{Sed.POc}})}{dz} \right]_{n_z=0} +$	$[mmol \text{ C m}^{-3}]$

	$\frac{1}{\text{REDF}_{\text{C},\text{O}_2}} \left[ \frac{\theta(-O_2)(\epsilon_{\text{Sed},\text{Anox}} C_{\text{Sed},\text{POC}})}{dz} \right]_{n_z=0}$	
$C_{\text{TA}}$ : total alkalinity	$R_{\text{TA}} = \frac{R_{\text{NH}_4}^* - R_{\text{NO}_3}^*}{\text{REDF}_{\text{C},\text{O}_2} \text{REDF}_{\text{C},\text{N}}} - 0.5 \times \theta(-O_2) R_{O_2} - \frac{R_{\text{PO}_4}^*}{\text{REDF}_{\text{C},\text{O}_2} \text{REDF}_{\text{C},\text{P}}} + \text{BottomTA}$ where terms with * exclude surface and bottom exchange fluxes	[mmol m <sup>-3</sup> ]
BottomTA: benthic-pelagic total alkalinity exchange flux	$\text{BottomTA} = \left[ \frac{\theta(O_2)(\epsilon_{\text{Sed},\text{Ox}} C_{\text{Sed},\text{PON}})}{dz \text{REDF}_{\text{C},\text{O}_2} \text{REDF}_{\text{C},\text{N}}} \right]_{n_z} + \left[ \frac{\theta(-O_2)(\epsilon_{\text{Sed},\text{Anox}} C_{\text{Sed},\text{PON}})}{dz \text{REDF}_{\text{C},\text{O}_2} \text{REDF}_{\text{C},\text{N}}} \right]_{n_z} + \left[ \frac{\theta(-O_2)\theta(NO_3)(a_{\text{denit}} \epsilon_{\text{Sed},\text{Anox}} C_{\text{Sed},\text{PON}})}{dz \text{REDF}_{\text{C},\text{O}_2} \text{REDF}_{\text{C},\text{N}}} \right]_{n_z} - 0.5 \times \theta(-O_2) \text{BottomO}_2$	[mmol m <sup>-3</sup> s <sup>-1</sup> ]

## References

- Aminot, A. and Kéruel, R.: Dissolved organic carbon, nitrogen and phosphorus in the N-E Atlantic and the N-W Mediterranean with particular reference to non-refractory fractions and degradation, Deep Sea Research Part I: Oceanographic Research Papers, 51, 1975–1999, <https://doi.org/10.1016/j.dsr.2004.07.016>, 2004.
- Blackford, J. C. and Gilbert, F. J.: pH variability and CO<sub>2</sub> induced acidification in the North Sea, Journal of Marine Systems, 64, 229–241, <https://doi.org/10.1016/j.jmarsys.2006.03.016>, 2007.
- Børshheim, K. Y., Vadstein, O., Myklestad, S. M., Reinertsen, H., Kirkvold, S., and Olsen, Y.: Photosynthetic algal production, accumulation and release of phytoplankton storage carbohydrates and bacterial production in a gradient in daily nutrient supply, Journal of Plankton Research, 27, 743–755, <https://doi.org/10.1093/plankt/fbi047>, 2005.
- Chaichana, S., Jickells, T., and Johnson, M.: Distribution and C/N stoichiometry of dissolved organic matter in the North Sea in summer 2011–12, Biogeosciences Discuss, 1–33, <https://doi.org/10.5194/bg-2017-387>, 2017.
- Chaichana, S., Jickells, T., and Johnson, M.: Interannual variability in the summer dissolved organic matter inventory of the North Sea: Implications for the continental shelf pump, Biogeosciences, 16, 1073–1096, <https://doi.org/10.5194/bg-16-1073-2019>, 2019.
- Church, M. J., Ducklow, H. W., and Karl, D. M.: Multiyear increases in dissolved organic matter inventories at Station ALOHA in the North Pacific Subtropical Gyre, Limnology and Oceanography, 47, 1–10, <https://doi.org/10.4319/lo.2002.47.1.0001>, 2002.
- Clark, L. L., Ingall, E. D., and Benner, R.: Marine phosphorus is selectively remineralized, Nature, 393, 426–426, <https://doi.org/10.1038/30881>, 1998.
- Daewel, U. and Schrum, C.: Simulating long-term dynamics of the coupled North Sea and Baltic Sea ecosystem with ECOSMO II: Model description and validation, Journal of Marine Systems, 119–120, 30–49, <https://doi.org/10.1016/j.jmarsys.2013.03.008>, 2013.
- Davis, C. E., Mahaffey, C., Wolff, G. A., and Sharples, J.: A storm in a shelf sea: Variation in phosphorus distribution and organic matter stoichiometry, Geophysical Research Letters, 41, 8452–8459, <https://doi.org/10.1002/2014GL061949>, 2014.
- Davis, C. E., Blackbird, S., Wolff, G., Woodward, M., and Mahaffey, C.: Seasonal organic matter dynamics in a temperate shelf sea, Progress in Oceanography, 177, <https://doi.org/10.1016/j.pocean.2018.02.021>, 2019.

Doval, M. D., Pérez, F. F., and Berdalet, E.: Dissolved and particulate organic carbon and nitrogen in the Northwestern Mediterranean, Deep Sea Research Part I: Oceanographic Research Papers, 46, 511–527, [https://doi.org/10.1016/S0967-0637\(98\)00072-7](https://doi.org/10.1016/S0967-0637(98)00072-7), 1999.

Engel, A.: Direct relationship between CO<sub>2</sub> uptake and transparent exopolymer particles production in natural phytoplankton, Journal of Plankton Research, 24, 49–53, <https://doi.org/10.1093/plankt/24.1.49>, 2002.

Fajon, C., Cauwet, G., Lebaron, P., Terzic, S., Ahel, M., Malej, A., Mozetic, P., and Turk, V.: The accumulation and release of polysaccharides by planktonic cells and the subsequent bacterial response during a controlled experiment, FEMS Microbiology Ecology, 29, 351–363, [https://doi.org/10.1016/S0168-6496\(99\)00029-X](https://doi.org/10.1016/S0168-6496(99)00029-X), 1999.

Frigstad, H., Andersen, T., Hessen, D. O., Jeansson, E., Skogen, M., Naustvoll, L.-J., Miles, M. W., Johannessen, T., and Bellerby, R. G. J.: Long-term trends in carbon, nutrients and stoichiometry in Norwegian coastal waters: Evidence of a regime shift, Progress in Oceanography, 111, 113–124, <https://doi.org/10.1016/j.pocean.2013.01.006>, 2013.

Hansell, D. A. and Carlson, C. A.: Deep-ocean gradients in the concentration of dissolved organic carbon, Nature, 395, 263–266, <https://doi.org/10.1038/26200>, 1998.

Hoikkala, L., Lahtinen, T., Perttilä, M., and Lignell, R.: Seasonal dynamics of dissolved organic matter on a coastal salinity gradient in the northern Baltic Sea, Continental Shelf Research, 45, 1–14, <https://doi.org/10.1016/j.csr.2012.04.008>, 2012.

Hoikkala, L., Kortelainen, P., Soinne, H., and Kuosa, H.: Dissolved organic matter in the Baltic Sea, Journal of Marine Systems, 142, 47–61, <https://doi.org/10.1016/j.jmarsys.2014.10.005>, 2015.

Hopkinson, C. S. and Vallino, J. J.: Efficient export of carbon to the deep ocean through dissolved organic matter, Nature, 433, 142–145, <https://doi.org/10.1038/nature03191>, 2005.

Hopkinson, C. S., Fry, B., and Nolin, A. L.: Stoichiometry of dissolved organic matter dynamics on the continental shelf of the northeastern U.S.A., 17, 473–489, [https://doi.org/10.1016/S0278-4343\(96\)00046-5](https://doi.org/10.1016/S0278-4343(96)00046-5), 1997.

Hopkinson, C. S., Vallino, J. J., and Nolin, A.: Decomposition of dissolved organic matter from the continental margin, Deep Sea Research Part II: Topical Studies in Oceanography, 49, 4461–4478, [https://doi.org/10.1016/S0967-0645\(02\)00125-X](https://doi.org/10.1016/S0967-0645(02)00125-X), 2002.

Huang, J.: A Simple Accurate Formula for Calculating Saturation Vapor Pressure of Water and Ice, Journal of Applied Meteorology and Climatology, 57, 1265–1272, <https://doi.org/10.1175/JAMC-D-17-0334.1>, 2018.

Humphreys, M. P., Lewis, E. R., Sharp, J. D., and Pierrot, D.: PyCO2SYS v1.8: marine carbonate system calculations in Python, *Geoscientific Model Development*, 15, 15–43, <https://doi.org/10.5194/gmd-15-15-2022>, 2022.

Humphreys, M. P., Schiller, A. J., Sandborn, D., Gregor, L., Pierrot, D., van Heuven, S. M. A. C., Lewis, E. R., and Wallace, D. W. R.: PyCO2SYS: marine carbonate system calculations in Python, , <https://doi.org/10.5281/zenodo.10671397>, 2024.

Hung, J.-J., Chen, C.-H., Gong, G.-C., Sheu, D.-D., and Shiah, F.-K.: Distributions, stoichiometric patterns and cross-shelf exports of dissolved organic matter in the East China Sea, *Deep Sea Research Part II: Topical Studies in Oceanography*, 50, 1127–1145, [https://doi.org/10.1016/S0967-0645\(03\)00014-6](https://doi.org/10.1016/S0967-0645(03)00014-6), 2003.

Hung, J.-J., Wang, S.-M., and Chen, Y.-L.: Biogeochemical controls on distributions and fluxes of dissolved and particulate organic carbon in the Northern South China Sea, *Deep Sea Research Part II: Topical Studies in Oceanography*, 54, 1486–1503, <https://doi.org/10.1016/j.dsr2.2007.05.006>, 2007.

Kim, T.-H. and Kim, G.: Factors controlling the C:N:P stoichiometry of dissolved organic matter in the N-limited, cyanobacteria-dominated East/Japan Sea, *Journal of Marine Systems*, 115–116, 1–9, <https://doi.org/10.1016/j.jmarsys.2013.01.002>, 2013.

Kossack, J., Mathis, M., Daewel, U., Liu, F., Demir, K. T., Thomas, H., and Schrum, C.: Tidal impacts on air-sea CO<sub>2</sub> exchange on the North-West European shelf, *Front. Mar. Sci.*, 11, 1406896, <https://doi.org/10.3389/fmars.2024.1406896>, 2024.

Letscher, R. T. and Moore, J. K.: Preferential remineralization of dissolved organic phosphorus and non-Redfield DOM dynamics in the global ocean: Impacts on marine productivity, nitrogen fixation, and carbon export, *Global Biogeochemical Cycles*, 29, 325–340, <https://doi.org/10.1002/2014GB004904>, 2015.

Letscher, R. T., Moore, J. K., Teng, Y.-C., and Primeau, F.: Variable C : N : P stoichiometry of dissolved organic matter cycling in the Community Earth System Model, *Biogeosciences*, 12, 209–221, <https://doi.org/10.5194/bg-12-209-2015>, 2015.

Liang, Z., Letscher, R. T., and Knapp, A. N.: Global Patterns of Surface Ocean Dissolved Organic Matter Stoichiometry, *Global Biogeochemical Cycles*, 37, e2023GB007788, <https://doi.org/10.1029/2023GB007788>, 2023.

Loh, A. N. and Bauer, J. E.: Distribution, partitioning and fluxes of dissolved and particulate organic C, N and P in the eastern North Pacific and Southern Oceans, *Deep Sea Res. Pt. I*, 47, 2287–2316, [https://doi.org/10.1016/S0967-0637\(00\)00027-3](https://doi.org/10.1016/S0967-0637(00)00027-3), 2000.

Lønborg, C. and Álvarez-Salgado, X. A.: Recycling versus export of bioavailable dissolved organic matter in the coastal ocean and efficiency of the continental shelf pump, *Global Biogeochemical Cycles*, 26, GB3018, <https://doi.org/10.1029/2012GB004353>, 2012.

Lønborg, C., Carreira, C., Abril, G., Agustí, S., Amaral, V., Andersson, A., Arístegui, J., Bhadury, P., Bif, M. B., Borges, A. V., Bouillon, S., Calleja, M. L., Cotovicz Jr., L. C., Cozzi, S., Doval, M., Duarte, C. M., Eyre, B., Fichot, C. G., García-Martín, E. E., Garzon-Garcia, A., Giani, M., Gonçalves-Araujo, R., Gruber, R., Hansell, D. A., Hashihama, F., He, D., Holding, J. M., Hunter, W. R., Ibánhez, J. S. P., Ibello, V., Jiang, S., Kim, G., Klun, K., Kowalcuk, P., Kubo, A., Lee, C.-W., Lopes, C. B., Maggioni, F., Magni, P., Marrase, C., Martin, P., McCallister, S. L., McCallum, R., Medeiros, P. M., Morán, X. A. G., Muller-Karger, F. E., Myers-Pigg, A., Norli, M., Oakes, J. M., Osterholz, H., Park, H., Lund Paulsen, M., Rosentreter, J. A., Ross, J. D., Rueda-Roa, D., Santinelli, C., Shen, Y., Teira, E., Tinta, T., Uher, G., Wakita, M., Ward, N., Watanabe, K., Xin, Y., Yamashita, Y., Yang, L., Yeo, J., Yuan, H., Zheng, Q., and Álvarez-Salgado, X. A.: A global database of dissolved organic matter (DOM) concentration measurements in coastal waters (CoastDOM v1), *Earth System Science Data*, 16, 1107–1119, <https://doi.org/10.5194/essd-16-1107-2024>, 2024.

Lucea, A., Duarte, C. M., Agustí, S., and Søndergaard, M.: Nutrient (N, P and Si) and carbon partitioning in the stratified NW Mediterranean, *Journal of Sea Research*, 49, 157–170, [https://doi.org/10.1016/S1385-1101\(03\)00005-4](https://doi.org/10.1016/S1385-1101(03)00005-4), 2003.

Martiny, A. C., Vrugt, J. A., and Lomas, M. W.: Concentrations and ratios of particulate organic carbon, nitrogen, and phosphorus in the global ocean, *Sci Data*, 1, 140048, <https://doi.org/10.1038/sdata.2014.48>, 2014.

Nausch, M., Nausch, G., Wasmund, N., and Nagel, K.: Phosphorus pool variations and their relation to cyanobacteria development in the Baltic Sea: A three-year study, *Journal of Marine Systems*, 71, 99–111, <https://doi.org/10.1016/j.jmarsys.2007.06.004>, 2008.

Neumann, T., Radtke, H., Cahill, B., Schmidt, M., and Rehder, G.: Non-Redfieldian carbon model for the Baltic Sea (ERGOM version 1.2) – implementation and budget estimates, *Geosci. Model Dev.*, 15, 8473–8540, <https://doi.org/10.5194/gmd-15-8473-2022>, 2022.

Osterholz, H., Burmeister, C., Busch, S., Dierken, M., Frazão, H. C., Hansen, R., Jeschek, J., Kremp, A., Kreuzer, L., Sadkowiak, B., Waniek, J. J., and Schulz-Bull, D. E.: Nearshore Dissolved and Particulate Organic Matter Dynamics in the Southwestern Baltic Sea: Environmental Drivers and Time Series Analysis (2010–2020), *Frontiers in Marine Science*, 8:795028, <https://doi.org/10.3389/fmars.2021.795028>, 2021.

Painter, S. C., Hartman, S. E., Kivimäe, C., Salt, L. A., Clargo, N. M., Daniels, C. J., Bozec, Y., Daniels, L., Allen, S., Hemsley, V. S., Moschonas, G., and Davidson, K.: The elemental stoichiometry (C, Si, N, P) of the Hebrides Shelf and its role in carbon export, *Progress in Oceanography*, 159, 154–177, <https://doi.org/10.1016/j.pocean.2017.10.001>, 2017.

Painter, S. C., Lapworth, D. J., Woodward, E. M. S., Kroeger, S., Evans, C. D., Mayor, D. J., and Sanders, R. J.: Terrestrial dissolved organic matter distribution in the North Sea, *Science of The Total Environment*, 630, 630–647, <https://doi.org/10.1016/j.scitotenv.2018.02.237>, 2018.

Pujo-Pay, M., Conan, P., Oriol, L., Cornet-Barthaux, V., Falco, C., Ghiglione, J.-F., Goyet, C., Moutin, T., and Prieur, L.: Integrated survey of elemental stoichiometry (C, N, P) from the western to eastern Mediterranean Sea, *Biogeosciences*, 8, 883–899, <https://doi.org/10.5194/bg-8-883-2011>, 2011.

Raimbault, P., Pouvesle, W., Diaz, F., Garcia, N., and Sempéré, R.: Wet-oxidation and automated colorimetry for simultaneous determination of organic carbon, nitrogen and phosphorus dissolved in seawater, *Marine Chemistry*, 66, 161–169, [https://doi.org/10.1016/S0304-4203\(99\)00038-9](https://doi.org/10.1016/S0304-4203(99)00038-9), 1999.

Redfield, A. C.: The influence of organisms on the composition of seawater, *The sea*, 2, 26–77, 1963.

Rowe, O. F., Dinasquet, J., Paczkowska, J., Figueroa, D., Riemann, L., and Andersson, A.: Major differences in dissolved organic matter characteristics and bacterial processing over an extensive brackish water gradient, the Baltic Sea, *Marine Chemistry*, 202, 27–36, <https://doi.org/10.1016/j.marchem.2018.01.010>, 2018.

Santinelli, C., Ibello, V., Lavezza, R., Civitarese, G., and Seritti, A.: New insights into C, N and P stoichiometry in the Mediterranean Sea: The Adriatic Sea case, *Continental Shelf Research*, 44, 83–93, <https://doi.org/10.1016/j.csr.2012.02.015>, 2012.

Singh, A., Baer, S. E., Riebesell, U., Martiny, A. C., and Lomas, M. W.: C : N : P stoichiometry at the Bermuda Atlantic Time-series Study station in the North Atlantic Ocean, *Biogeosciences*, 12, 6389–6403, <https://doi.org/10.5194/bg-12-6389-2015>, 2015.

Søndergaard, M., Williams, P. J. le B., Cauwet, G., Riemann, B., Robinson, C., Terzic, S., Woodward, E. M. S., and Worm, J.: Net accumulation and flux of dissolved organic carbon and dissolved organic nitrogen in marine plankton communities, *Limnology and Oceanography*, 45, 1097–1111, <https://doi.org/10.4319/lo.2000.45.5.1097>, 2000.

Stepanauskas, R., JØrgensen, N. O. G., Eigaard, O. R., Žvikas, A., Tranvik, L. J., and Leonardson, L.: Summer Inputs of Riverine Nutrients to the Baltic Sea: Bioavailability and Eutrophication Relevance, *Ecological Monographs*, 72, 579–597, [https://doi.org/10.1890/0012-9615\(2002\)072\[0579:SIORNT\]2.0.CO;2](https://doi.org/10.1890/0012-9615(2002)072[0579:SIORNT]2.0.CO;2), 2002.

Suratman, S., Weston, K., Jickells, T., and Fernand, L.: Spatial and seasonal changes of dissolved and particulate organic C in the North Sea, *Hydrobiologia*, 628, 13–25, <https://doi.org/10.1007/s10750-009-9730-z>, 2009.

Tanioka, T., Matsumoto, K., and Lomas, M. W.: Drawdown of Atmospheric pCO<sub>2</sub> Via Variable Particle Flux Stoichiometry in the Ocean Twilight Zone, *Geophysical Research Letters*, 48, e2021GL094924, <https://doi.org/10.1029/2021GL094924>, 2021.

Tanioka, T., Larkin, A. A., Moreno, A. R., Brock, M. L., Fagan, A. J., Garcia, C. A., Garcia, N. S., Gerace, S. D., Lee, J. A., Lomas, M. W., and Martiny, A. C.: Global Ocean Particulate Organic Phosphorus, Carbon, Oxygen for Respiration, and Nitrogen (GO-POPCORN), *Sci Data*, 9, 688, <https://doi.org/10.1038/s41597-022-01809-1>, 2022.

Thomas, H., Ittekkot, V., Osterroht, C., and Schneider, B.: Preferential recycling of nutrients—the ocean’s way to increase new production and to pass nutrient limitation?, *Limnology and Oceanography*, 44, 1999–2004, <https://doi.org/10.4319/lo.1999.44.8.1999>, 1999.

Voss, M., Asmala, E., Bartl, I., Carstensen, J., Conley, D. J., Dippner, J. W., Humborg, C., Lukkari, K., Petkuviene, J., Reader, H., Stedmon, C., Vybernaite-Lubiene, I., Wannicke, N., and Zilius, M.: Origin and fate of dissolved organic matter in four shallow Baltic Sea estuaries, *Biogeochemistry*, 154, 385–403, <https://doi.org/10.1007/s10533-020-00703-5>, 2021.

Williams, P. M., Carlucci, A. F., and Olson, R.: A deep profile of some biologically important properties in the central North Pacific gyre, *Oceanologica Acta*, 3, 471–476, <https://archimer.ifremer.fr/doc/00122/23291/21119.pdf>, 1980.

Winogradow, A., Mackiewicz, A., and Pempkowiak, J.: Seasonal changes in particulate organic matter (POM) concentrations and properties measured from deep areas of the Baltic Sea, *Oceanologia*, 61, 505–521, <https://doi.org/10.1016/j.oceano.2019.05.004>, 2019.